Università degli Studi di Torino
Doctoral School of the University of Torino
PhD Programme in Chemical and Materials Sciences XXXV Cycle

Isolation of high-added value products by extraction in supercritical CO_2 and relative characterization

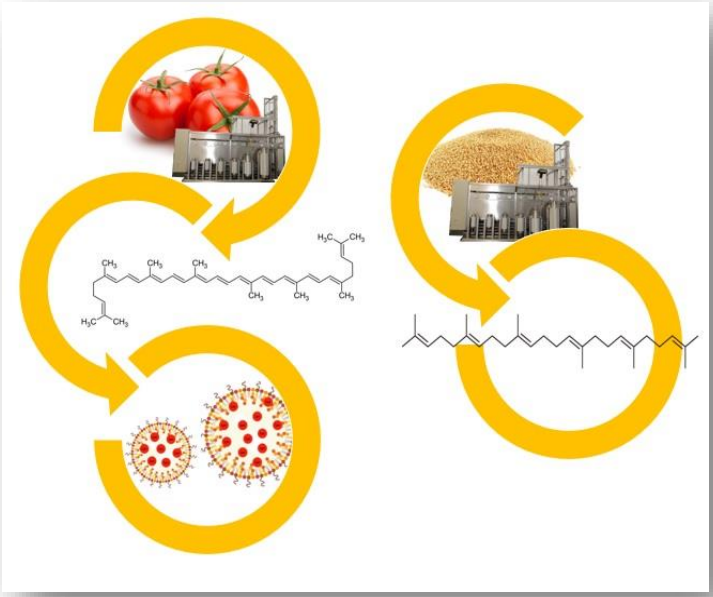

Chiara Cavagnero

Supervisor: Prof. Guido Viscardi

Università degli Studi di Torino

Doctoral School of the University of Torino

PhD Programme in Chemical and Materials Sciences XXXV cycle

Isolation of high-added value products by extraction in supercritical CO_2 and relative characterization

Candidate: **Chiara Cavagnero**

Supervisor: Prof. **Guido Viscardi**

Jury Members:

Prof. **Pierluigi Quagliotto**
University di Torino
Department of Chemistry

Prof. **Graciela Pavon-Djavid**
University of Sorbonne Paris Nord
Laboratory for Vascular Translational Science, Cardiovascular Bioengineering

Prof. **Riccardo Leardi**
University of Genova
Department of Pharmacy

Head of the Doctoral School: Prof. Alberto Rizzuti
PhD Programme Coordinator: Prof. Bartolomeo Civalleri

Torino, 16th December 2022

Index

Introduction.

Since the beginning of human history, women and men have always explored plant species to improve their health (Borges Silva et al., 2018). At first the plant kingdom was used mainly for food purposes, later, with the advent of (modern) technological progress, it was also understood that plants can be an important source of chemical compounds which have positive biological effects on human health (Gullon et al., 2020). These very useful substances can be localized in all of a plant's different physiological structures, starting from the roots and then up to the leaves (Fang et al., 2019). The biological effect of a chemical compound is strongly correlated with its quantity in the matrix, so it is important to know it within the plant material (Chemat et al., 2017).

In pharmacological, and in particular phyto-therapeutic applications, the quantity of an active principle compared to the matrix total amount plays a major role since it can determine the different effect that the substance has on the study model, both for its intrinsic interaction but also for the quantity of matrix that needs to be used to reach an appropriate value of a specific molecule. The higher the content of a specific substance in the matrix is, the less matrix is needed to be used to reach a certain product quantity. Thanks to improvements in technology over the last two centuries, it has been possible to quantify bioactive substance quantity in the plant kingdom. It turns out that they are low in dry weight terms and therefore a suitably effective doses of these substances cannot depend exclusively on the intake related to the plant matrix. To reach an appropriate quantity of a drug, the plant portions, or organs richest in the molecules of interest have been selected. The processes of purification by extraction have been performed on the latter to increase the concentration of the drug. In this way it is possible to obtain discrete concentrated bioactive chemical compound quantities without using the entire plant (Mariatti et al., 2021).

Several extraction techniques have been developed, but always with the same basic principles. Each extraction procedure is composed of several steps (Jiang et al., 2021):

- Selection of a suitable matrix with the highest content of the product of interest in order to minimize the amount of raw material used.
- Selection of a solvent able to solubilize the substance of interest as selectively as possible.

- Promotion if the solvent penetration into the matrix to solubilize the substance; usually through pre-treatments performed at matrix level such as removing water by drying or increasing the surface volume ration by grinding.
- Obtaining the solution composed of solvent and solutes exhaustively, safely and continuously.
- Removing the solvent to obtain a product that is as concentrated as possible, usually through post-treatments operated at the extraction level such as evaporation or filtration.

Many of these techniques have proved their efficiency in terms of performance and remuneration, and over the last fifty years these methods have been overused, even if most of them are not environmentally sustainable, mainly for two reasons (Picot-Allain et al., 2021):

- Most of the solvents used are non-polar such as hexane, dichloromethane, acetone, or acetonitrile which are harmful to the environment as they can be poisonous, stinging, and carcinogenic for several animal species, including humans (Lomonaco et al., 2020). The disposal of these products must take place through special treatments that require high costs and complicated administrative procedures.
- The low quantities of substances within the plant matrices lead to the enormous waste of biomass. Often this waste might also be contaminated by solvents or denatured compounds and therefore can cause additional environmental problems and increased costs.

In the last thirty years public sensitivity to the environment and health began to cause first the research field, and later the industrial field, to modify the *modus operandi* of the extraction sector. The extraction procedures have been pushed towards increasingly green and eco-sustainable methods, based above all, on the principle of the circular economy (Armenta et al., 2019).

Green extraction is based on a process design that can reduce energy consumption, allow harmful solvent volume reduction, or lead to alternative solvent use ensuring a safe and high extract quality (de Jesus and Filho, 2020). This definition identifies the main idea of intensified extraction, therefore higher process quality by decreasing processed raw material, production waste and processing solvents, maximizing the

final extraction yield by reducing processing and management costs (de Melo et al., 2014).

This PhD work has its roots in the principle of Green Chemistry and aims to develop and improve the extraction process from vegetables and food waste materials using green extraction techniques. This project was developed by the Chemistry Department of Torino University side by side with the Exenia Group s.r.l., both with the intention of taking a step forward in improving green extraction technology. Exenia Group s.r.l. has had 25 years of experience with supercritical fluids by designing and developing pilot and industrial plants. On the other hand, the University of Turin has provided the expertise and advice thanks to its research experience and the connection with other research groups, such as the Pharmacy Department of Genova University and the Laboratoire de Recherche Vasculaire Translationnelle of Sorbonne University - Paris Nord, providing a new methodological approach and support with analytical techniques.

The present research project was kick-started by the market request for oil low in saturated fatty acids. For this reason, the first year was dedicated to the study of the extraction process of *Amaranthus cruentus*. From this cereal it is possible to obtain an oil rich in fatty acid, also containing biologically active molecules such as squalene. This process followed a univariate approach, exploring one variable at time, and led to an oil rich in squalene, and to a second fraction with a lower amount of squalene, but nonetheless usable in the cosmetic or food sector.

In the second year, the research moved to the valorisation of the waste material coming from the tomato paste industry. This waste is mainly made of tomato skins and seeds and can make up to between 10 to 30 % of the initial weight of the fresh tomatoes used, still containing however, an important fraction of bioactive compounds such as carotenoids, and in particular lycopene. The optimization of extraction with supercritical carbon dioxide followed a multivariate approach, since the number of experiments was limited due to lack of waste materials. Thanks to this, not only the influence of the extraction factor but also the characteristics of the waste have been possible to estimate. With this optimization process an oleoresin rich in lycopene was obtained, with carotenoids which are well known for their antioxidant activity, and commonly used in the fight against cardiovascular disease.

During the third year of the Doctorate, the research was developed in the Laboratory of the Sorbonne University, Paris Nord, initially through a characterization of the lycopene content of the oleoresin obtained by extraction with SC-CO_2 and its antioxidant activity. Another important goal was the synthesis of nanoparticles lipid carrier (NLCs). Lycopene is a C40 unsaturated hydrocarbon with 13 double bonds, 11 of which are conjugated. This configuration is responsible for its high antioxidant power, but at the same time it is also responsible for its high instability. For this reason, the NLCs have been synthesized to ensure the antioxidant activity of the oleoresin. The NLCs synthesis process was optimized by a multivariate approach, which allowed exploration of the impact of different experimental variables on the encapsulation rate and size distribution.

Chapter 1. Green extraction.

Introduction. In the phyto-pharmaceutical research field, the extraction of high-added value bioactive compounds from vegetable materials plays a major role (Pulok K. et al., 2019, pp. 237-328 and pp. 707-722) (M. Lu et al., 2019). To solubilize these chemicals it is essential that an appropriate solvent is used, with similar chemical properties. Traditionally, non-polar compounds are extracted by non-polar solvents such as hexane, benzene, and toluene. These solvents are dangerous for the environment and for the operators and, moreover, are difficult to remove from the final product as well as leaving harmful traces.

Over the centuries, extraction procedures have increasingly evolved, in particular those related to non-polar chemical compounds. If at first the extraction procedure was mainly operated by mechanical oil extraction using different press types, gradually more and more performing chemical methods ensured greater yields and more complete extractions, including the unsaponifiable component (Bhuiya et al., 2020). Furthermore, if it was possible to proceed mechanically only with extremely oily matrices, especially seeds, such as sunflower, rapeseed, corn or peanuts, or drupes such as olives, subsequently the complete lipid fraction could be obtained chemically using any plant matrix, including less oily seeds or, after drying, leaves, roots, fruits and flowers. This extraction method is defined as solid-liquid, since solutes are solubilized by means of a liquid solvent and are extracted from a solid inert matrix. When a solvent comes into contact with a solid matrix, which contains the solutes of interest, the following phenomena occur in sequence (Das and Arora, 2021):

1. Solvent diffusion from the solution to the matrix surface through the boundary layer. The boundary layer is defined as the solvent layer in direct contact with the matrix.
2. Solvent penetration inside the matrix through the micropores contained therein and forming a wetting phase within it. The wetting phase is defined as a liquid capable of penetrating inside solid matrices and dissolving solutes.
3. Solute solvation by the solvent. In this phase the solute concentration increases in the solvent, while it decreases inside the extractive matrix.
4. Concentration gradient formation within the solvent, relative to the solute. It is greater within the wetting phase and decreases as the solvent distance from the matrix increases.

5. Solute diffusion through the boundary layer in the entire solvent volume.

Diffusion stops when the concentration gradient is extinguished, and therefore when solute concentration in the wetting phase is the same as in the total solvent solution. At the end of this phase, the mechanical separation of the solution from the matrix usually takes place, through filtration or centrifugation (Bucić-Kojić et al., 2007). If, in this phase, it was possible to completely separate the solution from the matrix, all the solute would be extracted and the operation would thus be concluded with an extraction yield equal to 100%. However, there will always be a certain solution amount that will not be extracted, and therefore the extraction yield (solute amount extracted compared to solute initially present in the matrix) will be less than 100%. This also involves the exhausted matrix contamination and waste production that can no longer be used. To increase the extraction process yield, other extractions in series can be used, which however increase the amount of solvent used. This "solvent-diffusion-separation additions" sequence can be repeated as long as the extraction yield is considered suitable, and the solute amount dissolved in the wetting phase and in the matrix is tolerable. Solid-liquid extraction is the most widely used extraction method to obtain active compounds from plant matrices. Some of the most used classical procedures, even today, are the following:

- **Maceration**. It is an extraction technique that uses the direct contact between solid matrix and extractive solvent at room temperature able to solubilize the solutes of interest (Moharrami and Hashempour, 2021). Normally it is carried out inside chambers in which the matrix (often pre-treated with drying or milling processes) is immersed inside the solvent, for a time depending on various factors such as: mixture mechanical stirring, temperature, affinity between solvent and solute and matrix-solvent exchange surface (Wojdyło et al., 2021). The final product is called macerated. The most common variants of this procedure are infusion and decoction, and the differences are in solvent temperature and in the processing time (Lou et al., 2021). Infusion means a maceration carried out at temperatures higher than 35 °C. The process begins by immersing the extractive matrix inside the solvent already heated at these temperatures. The final product is called an infused. Decoction means a maceration carried out at room temperature, but gradually heated up in order to exceed 35 °C. The final product is called a decoction. The higher the solvent temperature, the more

the kinetic energy of the solvent molecules increases, which leads to a decrease in the solute's solvation times and therefore to a reduction in extraction times.

- **Percolation.** This is an extraction technique that uses gravitational acceleration to allow a slow liquid solvent movement within a porous matrix, through the micro-pores. In this way, solvation and solubilization of the solutes of interest occur within the solvent, which is collected with a separatory funnel. To decrease the process times, the thickness of the porous matrix layer can be decreased, or the process can be carried out under pressure, to increase the mixture fall speed. The final product is called percolate (Benincá et al., 2016).
- **Hydrodistillation**. It is one of the most used methods for the extraction of solutes from solid matrices and particularly used for essential oil extraction. This extraction process includes, as a first step, the immersion of the extractive matrix in water inside an extraction flask. The ratio between water and matrix must be appropriate and, if not properly calibrated, it can affect the extraction yield. Consequentially, the mixture of matrix and solvent is heated, until the solvent changes from liquid to gaseous state. The increase in temperature and the carrier action of water vapor allows the evaporation of the volatile solutes. The gaseous solution obtained will be cooled through a condenser and will return to the liquid state. Due to the difference in density, the biphasic water-oil solution obtained can be separated by means of a separating funnel, a Clevenger apparatus or other devices (Gavahian et al., 2020). The Clevenger apparatus is composed of three main parts: a heated round bottom flask in which the organic material is placed, a separator with a manual stopcock for separating the distilled solution and a condenser. Since the extraction solvent is water, it is assumed that many thermolabile components of essential oils can be collected without undergoing degradation processes due to the exceeding temperatures equal to 100 °C. The great limitation of this technology is the total polarity of the solvent, which does not allow a complete extraction of the most apolar solutes. For this purpose, the Soxhlet technology has been improved.
- **Hot continuous extraction**. This method uses continuous extraction cycles alternating with solvent purification by evaporation, to keep a low solute concentration in the solvent (Bukhanko et al., 2020). Therefore, high diffusivity gradient levels are maintained within the solvent and so, solvent volumes can be decreased. The most

common apparatus used for this kind of extraction is the Soxhlet, made by a distillation flask, in which the solvent is placed; an extraction chamber, in which the matrix is inserted through an appropriate support; a condenser, powered by water (Zygler et al., 2012). The process consists in the following steps. The matrix is placed inside the extraction chamber by inserting it into a paper thimble with low contaminant release. The solvent is heated inside the flask until it reaches the boiling point, and changes from liquid to the gaseous state. Solvent evaporates until it reaches the condenser. Upon contact with the condenser, finding a temperature below its boiling point, the solvent condenses in drops and starts to fall back on the matrix. The process is designed in such a way that the solvent drips cold onto the sample and falls back, enriched with solutes, into the flask below. By evaporating, the solvent is pure and therefore suitable to solubilize solutes again. By repeating these evaporation-condensation-extraction cycles for about 24 hours, a high extraction yield can be achieved, in the meantime reducing solvent volumes (Bukhanko et al., 2020).

The use of these extraction methods on a global scale, and the increase in number of different solvents employed for this kind of process, have led to a great expansion of the matrices used, and therefore to greater extractable chemical compounds, but at the same time have led to an increase in contaminated and no longer usable waste products (Özcan et al., 2019). For this reason, nowadays green and more performing technologies are used, in line with green chemistry and circular economy principles, such as microwave-assisted extraction (MAE), ultrasound-assisted extraction (UAE) and supercritical fluid extraction (SFE). With regard to the first two types of extraction, the greatest advantages are the reduction of extraction times and the reduction of solvent volumes. Both factors lead to lower production costs. On the other hand, at the end of the extraction, the exhausted extractive matrix will always be contaminated by traces of solvent, while with the supercritical technology (described more in deep in the following sections), in addition to the aforementioned advantages, there is also the production of non-contaminated solvent waste.

- **Microwave-assisted extraction** (MAE). It is a fast and efficient extraction technique based on the use of microwaves to heat the mixture consisting of extractive matrix and solvent in order to facilitate and speed up the solute extraction. Unlike traditional heat sources, which act on a surface, from which heat spreads to the

internal layers of the body by conduction and convection, a microwave heat source acts on the entire volume if this is considered homogeneous. Therefore, while with conventional heating some time is required to heat the vessel before the heat is transferred to the mixture and therefore to the matrix and the solvent, through the use of microwaves the solution is heated directly (Sparr Eskilsson and Björklund, 2000). Microwaves are non-ionizing radiations, with a frequency between 300 Mhz and 300 Ghz, capable of activating the rotational energy levels of the molecules. Microwave heating is based on the dipole rotation and ion conduction effects that microwaves exert on dipolar molecules and electrically charged molecules, respectively (Chan et al., 2011). Dipolar molecules such as water, characterized by one end with a positive electric charge and the other with a negative charge, are sensitive to the alternating electric field generated by microwaves. The electromagnetic field, by continuously changing its direction, causes molecular rotation (to align the own dipole with that of the electric field), resulting in a sudden heating of the matter. The heating is also due to a number of other physical factors such as frictional forces and ionic conduction. (Mandal and Tandey, 2016). Taking advantage of the extractive solution sudden heating, this extractive method induces solute desorption, their mass transfer from the matrix to the solvent and their solubilization in the solvent. Microwaves generated by a magnetron are focused directly on the sample or spread inside a cavity in which it is placed. Heating can be carried out in open containers equipped with refrigerant at atmospheric pressure or in closed containers under pressure. This technique is defined as assisted as there is always the presence of solvent, even if often in small volumes. For a correct extractive yield, polar solvents with high dielectric constants heat up quickly in the presence of electromagnetic fields, while non-polar solvents heat up with much more difficulty.

- **Ultrasound-assisted extraction** (UAE). As MAE, also this extraction technique is always coupled with the use of small amounts of solvents, but it exploits some physical properties of sound waves to increase the extraction yield and decrease extraction timing. Sound waves consist of mechanical vibrations and are mainly characterized by properties such as frequency, wavelength and intensity that describe their type and physical properties. The term ultrasound identifies all those sound frequencies that exceed the audible threshold of the human ear, which is 16 kHz, and have frequencies

that can even reach 200 MHz. For extraction purposes, the use of ultrasound is exploited as it induces both at solvent level, and at extractive matrix level, a phenomenon called cavitation (Vinatoru, 2015). The high frequency ultrasonic waves propagate through the solvent generating alternating cycles of high and low pressure, producing acoustic cavitation. This term identifies a physical phenomenon for which microscopic areas of a liquid solution are characterized by sudden increases and decreases in temperature and pressure that lead to the formation of unstable small bubbles. The collapse of these bubbles near the extractive matrix causes significant structural damage to the latter, generating effects such as surface peeling, erosion, sonoporation and destruction of the cellular membrane and or cellular wall in plant matrices. Furthermore, the implosion of cavitation bubbles in liquid media creates macro-turbulence and micro-mixing phenomena, which lead to the formation of convective micro-motions within the solution (Vinatoru et al., 2017). These phenomena, related to cavitation, lead to a greater porosity of the matrix, an increase in the kinetic energy of the solution, compression and decompression of the extractive matrix, which result in an easier and faster entry of the solvent into the matrix and therefore an intensification of solute mass transfer in the solvent.

1.1 Supercritical fluids. Exenia Group, the company sponsoring the present research project together with the Piedmont Region - Italy, is working on the extraction

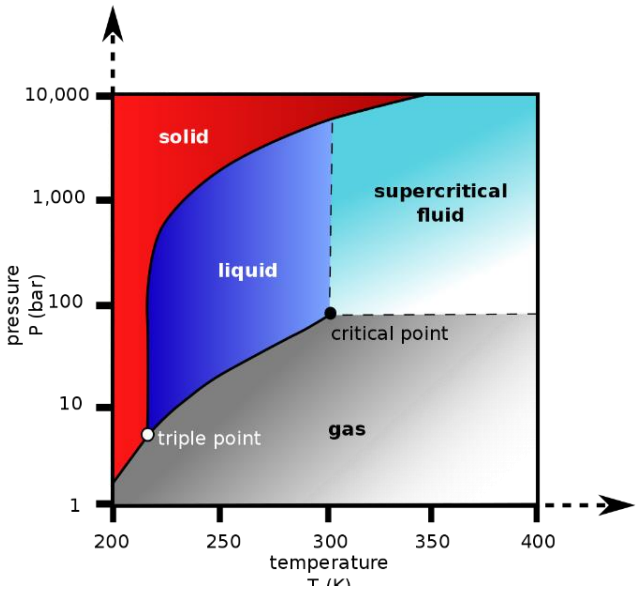

Figure 1. Carbon dioxide phase diagram.

by supercritical fluids from vegetable matrix since 1995. Supercritical fluid is any substance above its critical pressure and temperature, but below the pressure required to compress the substance into a solid, where a distinct liquid and gas phase does not exist (Schlosky, 1989). Supercritical fluid can effuse through a solid like a gas, overcoming the mass transfer limitation typical of a liquid. Close to the critical point, a small change in pressure and temperature drastically affects the density, comparable to the density on liquids. In particular, over the years, the Exenia Group has developed green extraction methods based on the use of carbon dioxide in a supercritical state as a solvent for the extraction of non-polar compounds.

1.2 Supercritical carbon dioxide. Carbon dioxide is a colourless gas, 60% more dense than dry air. It is composed of a carbon atom covalently double bonded with two oxygen atoms. In the pre-industrial era the concentration in the atmosphere was approximately 280 ppm lower than it is now (412 ppm) which resulted only from natural sources as volcanos, hot spring, geysers and from the dissolution of carbonate rocks in water. Nowadays, carbon dioxide finds a use in many fields, from soda preparation to fire extinguishers (Eggleton, 2013). Moreover, carbon dioxide is not a toxic substance and so it is accepted for contact with food and drug products both by the FDA (Food and Drug Administration) and EFSA (European Food Safety Authority).

The phase diagram of carbon dioxide in figure 1 shows some important data which helps us to understand why carbon dioxide is suitable to be used as a supercritical fluid. The well-known area of gas, liquid and solid states are showen respectively in grey, blue and red (figure 1), but with the increasing pressure and temperature, after the critical point, it's possible to find a light blue area where supercritical fluid can be observed. In figure 2, thanks to a specific pipe with a window resistant to high pressure, it is possible to observe the transition from a gas/liquid biphasic system to supercritical fluid monophase. Moving from right to left in fact, it is possible to see how the marked line that separates the two phases, liquid, and gas, start to be barely visible, and disappear in the last circle meaning that the supercritical state has been reached.

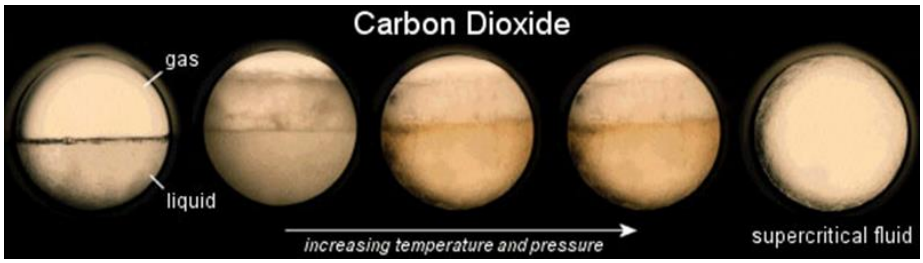

Figure 2. Transition from liquid-gas mixture to supercritical state.

Several substances show supercritical properties; the most common are reported in Table 1. For carbon dioxide the critical point is a relative very low pressure and temperature, so to obtain the supercritical state it is enough to reach 72,9 bar and 31,1°C. As a comparison, for water, the critical point is at 218,3 bar and 374,1°C, - a much higher value than for carbon dioxide, which makes prohibits the use of water in supercritical states for energy reasons. The low temperature value of supercritical carbon dioxide is also important in the extraction itself, as a matter of fact most compounds are sensitive to temperature and can degrade with heat. Supercritical carbon dioxide (SC-CO_2) can allow extraction at almost room temperature, so it is possible to extract thermolabile compounds. Another important property of carbon dioxide is that at room temperature and pressure is a gas as we can see in the phase diagram of figure 1.

Table 1. Value of critical temperature and pressure for different substances.

Solvent	T_c (°C)	p_c (atm)
CO_2	31.1	72.9
N_2O	36.5	71.7
$CHClF_2$ (Freon-22)	96	48.5
CHF_3 (Freon-23)	25.9	46.9
CH_3OH	240	78.5
i-C_3H_7OH	235.2	47
H_2O	374.1	218.3
SF_6	45.6	37
C_3H_8	96.7	41.9
n-C_6H_{14}	234.7	29.9

This is an advantage in the extraction process because a separation step after the extraction is no more needed. It is enough to low down pressure and temperature in an appropriate vessel to recover the extract.

SC-CO_2 is a perfect solvent for non-polar solutes. However, its use in combination with more polar solvents (ethanol or water), even in small amount, can improve the extraction capability for polar solutes as well. This kind of extraction shows several advantages compared to the classical techniques, because it is more eco-friendly and safer, no toxic solvents and no leaving of harmful traces, but it is also useful for thermolabile and/or oxidation sensible compounds.

Chapter 2. Methodology approach.

Introduction. Usually, scientists follow a univariate method to run their experiments, meaning that one variable is changed at time. A conventional approach in fact, after looking at previous work in the same field, would be to decide to start to run the experiments from a certain value of variables, and change the value of each variable one at time looking for the best response obtainable from a series of experiments. After choosing the value for the considered variable, a second variable is taken into consideration and again several experiments would be run to explore near close values, and see which one will give the best response. This process can be repeated until the last variable affecting the system has been altered. The results will be a value for each parameter considered in the examined process but we cannot be sure that these values are the ones giving the optimum for the system analysed, since they don't take into consideration the possible interaction between the variables.

2.1 Univariate approach. A univariate approach is commonly known as the one-factor-at-a-time method, or one-variable-at-a-time or monothetic analysis. It is a method of designing experiments involving the testing of factors, or causes, one at a time instead of multiple factors simultaneously. Usually, this approach it is favoured by non experts, especially in cases where the data can be obtained cheaply, and is abundant. Scientists used to thinking in a univariate way can find it difficult at the beginning to understand the potential of a multivariate approach. It may not be very intuitive at first glance.

2.2 Multivariate approach. The other extreme to univariate thought is the multivariate approach. At the base of this method it's possible to find multivariate statistics. This term is commonly used to identify the case in which multiple measurements are made on each experimental unit, and the relations among these measurements and their structures are important (Olkin and Sampson, 2001).

Nowadays an overlapping categorization of multivariate analysis includes:

- Normal and general multivariate models and distribution theory.
- The study and measurements of relationships.
- Probability computations of multidimensional regions.
- The exploration of data structures and patterns.

Cases exist where the mental effort required to conduct a complex multi-factor analysis exceeds the effort required to acquire the extra data. In this case, a one factor at time approach might make more sense. Further to this, under certain conditions (like when the number of runs is limited, and the primary goal is to attain improvements in the system, and experimental error is not large compared to factor effects, which must be additive and independent of each other), research (Friedman and Savage, 1947) (Daniel, 1973) has shown that a one factor at time approach might be more effective that fractional factorials.

On the other hand, there are some cases where data is precious because not as many experiments as would be wanted can be run, for both economic reasons as well as issues with supplies. In these cases, it is almost always better to change multiple factors at once.

The disadvantages of one factor at a time can be summarized in the following list:

- One factor at time requires more experiments to reach the same precision in effect estimation.
- One factor at time doesn't take into consideration the possible interaction between variables and so it isn't possible to estimate them with this approach; interaction can pay a substantial role in the optimization process.
- With one factor at time approach, it's easier to miss the variable value that returns the optimal zone for observed responses.

In conclusion, the multivariate approach remains nearly always preferred over the univariate approach with many types and methods available (Czitrom, 1999).

The design of experiments (DOE) is a methodology leading to design any task with the aim of describing and explaining the variation of information under certain conditions that are hypothesized to reflect the variation. The methodology is commonly used with experiments in which the design introduces conditions that directly affects the variation, however it can be applied to quasi-experiments, in which natural conditions influence the variation, and so they are selected for observation.

Usually, any experiment is run to predict the result by introducing a change of the preconditions, which are represented through independent variables. These variables are generally called "input variables" or "predictor variables". They are the ones that the scientist in question thinks that might affect the system by their variation or even

their presence at a certain value. Actually, the variable involved in an experimental design can also be "control variable", meaning a variable that must be held constant to prevent the possibility that external factors may affect the system. Last but not least, the scientist also needs to point out dependent variables, also referred to as "output variable" or "response variable" – that is, the variable that represents the response of the system at certain variation of the input variable.

In conclusion, it can be said that Experimental Design involves not only the selection of suitable independent, dependent, and control variables, but planning the delivery of the experiments under statistically optimal conditions given the constraints of available resources. There are multiple approaches for determining the set of design points (unique combinations of the settings of the independent variables) to be used in the experiment. One of the main concerns about Experimental Design is the establishment of validity, reliability, and replicability. However, these concerns can be partially minimized by carefully choosing the variables and reducing measurement errors. Nowadays, the design of experiments plays a major role in natural and social science but can be also applied to marketing for example.

Experimental design has deep historical roots. A methodology for designing experiments was proposed by Ronald Fisher in his innovative books: The Arrangement of Field Experiments (1926) and The Design of Experiments (1935). Much of his pioneering work dealt with agricultural applications of statistical methods.

The application of the multivariate approach, and so of the design of experiment methodology in chemistry is studied by the Chemometrics. Chemometrics is applied to solve both descriptive and predictive problems not only in chemistry but more in general in experimental natural sciences. Chemometrics can be applied in descriptive application, properties of systems are modelled to learn the underlying relationship and structure of the system, or in predictive application, properties of systems are modelled with the intent of predicting new properties or behaviour.

Chapter 3. Amaranthus cruentus.

Introduction. The market for seed oils obtained through a green extraction, like cold pressing or supercritical fluid extraction, is getting larger day by day. The most popular products at a large-scale distribution level are grape and apple seed oil. Other important products worth mentioning are pomegranate, flax, and pumpkin seed oils (Ferrentino et al., 2020). They are highly recommended for a diet low in saturated fatty acids. In fact, these oils are mainly made of mono or polyunsaturated fatty acids and the unsaponifiable component is characterized by high levels of tocopherols and some cholesterol-lowering substances such as phytosterols or squalene.

Amaranth is a plant native to South America. Historically is has been cultivated by the pre-Columbian populations between Bolivia and Perù. The edible species mostly used for food production are: *Amaranthus caudatus*, *Amaranthus cruentus* and *Amaranthus hypochondriacus*. It's a cereal without gluten containing an interesting oil fraction with important properties, like high level of tocopherols and squalene in its unsaponifiable fraction. It is one of the products with an ever-increasing consumer demand (M. Micera, et al., 2020).

Amaranth seeds contain oil rich of fatty acid for almost 75% composed of mono or polyunsaturated fatty acids (Zhang et al., 2019). In particular, linoleic acid counts for almost 40%, and oleic acid, for almost 20% of the total. On the other hand, saturated fatty acids, including palmitic and stearic acid, are found at low levels. The unsaponifiable fraction is also interesting, since it is rich in tocopherols, phytosterols and squalene - a triterpene molecule well-known for its antioxidant and anti-hypercholesterolemic activities, widely used in anti-aging cream formulations (Chen et al., 2021).

Recent studies showed that reducing saturated fatty acid consumption is beneficial for people affected by cardiovascular diseases, which are, in developed countries, the one of the main causes of death (Peltola et al., 2006). In this background, the oil extracted from *Amaranthus cruentus* with supercritical carbon dioxide plays an important rolein this. In fact, an increased use of unsaturated fats is of great benefit for cardiovascular problems and can also prevent cardiovascular diseases. An appropriate dietary amaranth oil consumption can lower blood cholesterol levels in murine animal models, an effect probably related to its squalene and polyunsaturated

fatty acid content. This observation is supported by the study of He et al., 2002, in which some hamsters were treated with hypercholesterolemic diets and amaranth oil (5%), and the results showed a significant decrease in blood cholesterol (-20%), compared to the group treated with hypercholesterolemic diets (He et al., 2002).

Lead by this request from the market, in the first year of the doctorate project the research activity was focused on the *Amaranthus cruentus* seeds as raw material. The experimental activity followed a classical univariate approach and was finalized to explore the parameters of the SC-CO_2 based extraction process able to give the highest yield in oil with the highest content in squalene from *Amaranthus cruentus* seeds as raw material.

3.1 Materials.

Amaranthus cruentus seeds were purchased from Padovana Macinazione S.r.l. (Padova, Italy). They were harvested in Perù and Bolivia and showed a size between 0.3 and 0.5 cm, and residual humidity less than 14%. The seeds were pre-treated by drying at 65 °C for 4 h, and then milled with a Novital mill before extraction; one single one batch has been considered. Flour with a particle size between 0.15 and 0.3 mm was obtained. Food grade carbon dioxide, purity > 99.98%, was purchased from Nippon Gases S.r.l.. HPLC grade solvents and squalene were purchased from Merck KGaA.

3.2 Methods.

SC-CO_2 Extraction. The first three months of the doctorate were involved in acquiring confidence and management skills needed to run the pilot extraction plant at the Exenia Group, working with SC-CO_2 in Pinerolo (TO). Figure 3 shows a photo of the plant used in this work while in figure 4 the scheme of the same plant developed by Exenia Group for extraction with SC-CO_2 is reported. Liquid carbon dioxide is transferred from a series of cylinders (upper left corner) in a refrigerated thank (S) through a cooled condenser (C) to ensure the liquid state of carbon dioxide.

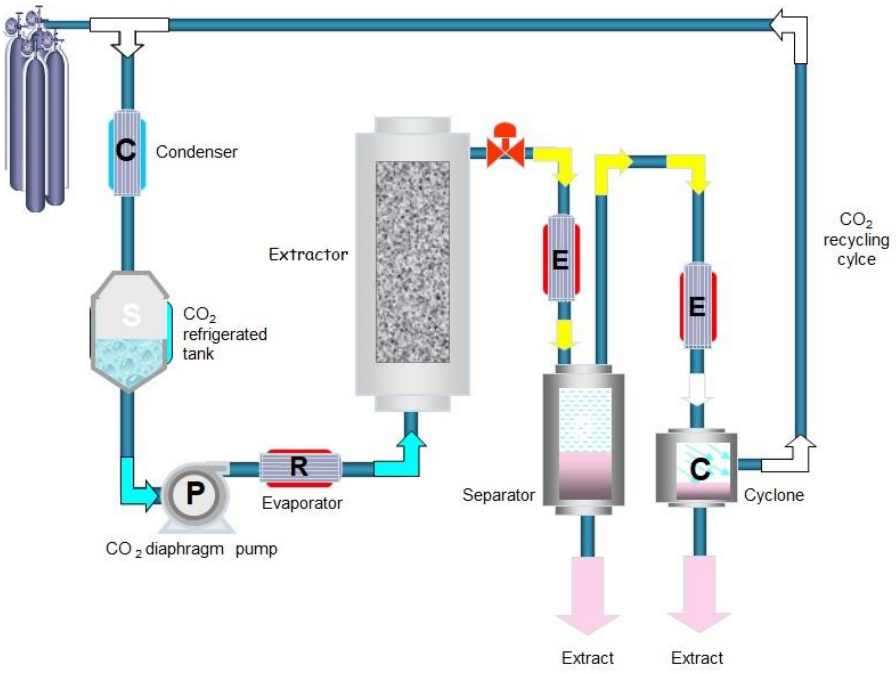

Figure 3. Scheme of the Exenia plant for extraction with supercritical carbon dioxide.

The liquid CO_2 is pumped at critical pressure by a diaphragm pump (P), and heated to critical temperature through a heat exchanger (R). After this step, the carbon dioxide is in supercritical state. The SC-CO_2 goes through the raw material, previously loaded in the extractor thanks to a specific basket. Looking at the parts coloured red in the diagram above, it's possible to note the back-pressure valve that is responsible for lowering the pressure; in this way the CO_2 becomes gaseous. A heat exchanger (E) compensates the sudden drop in temperature caused by Joule-Thompson effect. The flow of gaseous CO_2 with the dissolved extract goes through a series of separators with a different configuration so it is possible to separate the gaseous CO_2 from the extracted material. After all the separators, the carbon dioxide is cooled down so it returns to the liquid phase and can be stocked back in the tank.

Figure 4. The Exenia plant used for extraction with supercritical carbon dioxide.

The quantity of *Amaranthus cruentus* seeds as a raw material has been fixed at 2,5 kg, and the solvent flow at 18 kg/h. It the 5L vessel volume extractor was used, and the extract was collected from the first gravimetric separator. Minimal and uninteresting material was collected from the two cyclonic separators. Temperature, pressure, and extraction time were optimized following a univariate approach to optimize oil yield and cost of extraction process. For each point a minimum of three repetitions were performed.

HPLC analysis. HPLC analysis was performed with quaternary Flexar pump, manual injection valve with a 20 µL loop, Perkin Elmer column oven, Perkin Elmer PDA Plus detector (Perkin Elmer). Reverse phase C18 Pronto SIL column (250x4,6mm, 5µm). The HPLC conditions were as follows: A-MeOH, B-ACN: Gradient elution: 50% A 7min, 100% A 5 min, 100% A 3 min, 50% A 12 min, 50% A 25 min: flow: 1 ml\min: detection wavelength 210 nm. Injection volume: 20 µL. Standard solutions were prepared by dissolving 0.105 and 0.215 g of SQ in dichloromethane. After a 1:100

dilution in a 50:50 (v/v) solution of MeOH and ACN, a series of other dilutions were performed to obtain a range between 0.01 and 0.2 g/L. Squalene peak area was plotted vs actual concentrations to obtain a calibration curve (y= $1*10^8$ x) (*Figure 6*) with a linearity confirmed by the evaluation of determination coefficient (R2=0.9982). Samples were prepared as follows: 0.1 g solubilized in 9.9 mL of dichloromethane and then diluted 1:100 in a 50:50 (v/v) solution of MeOH and ACN. Twenty µL of this solution were injected for analysis.

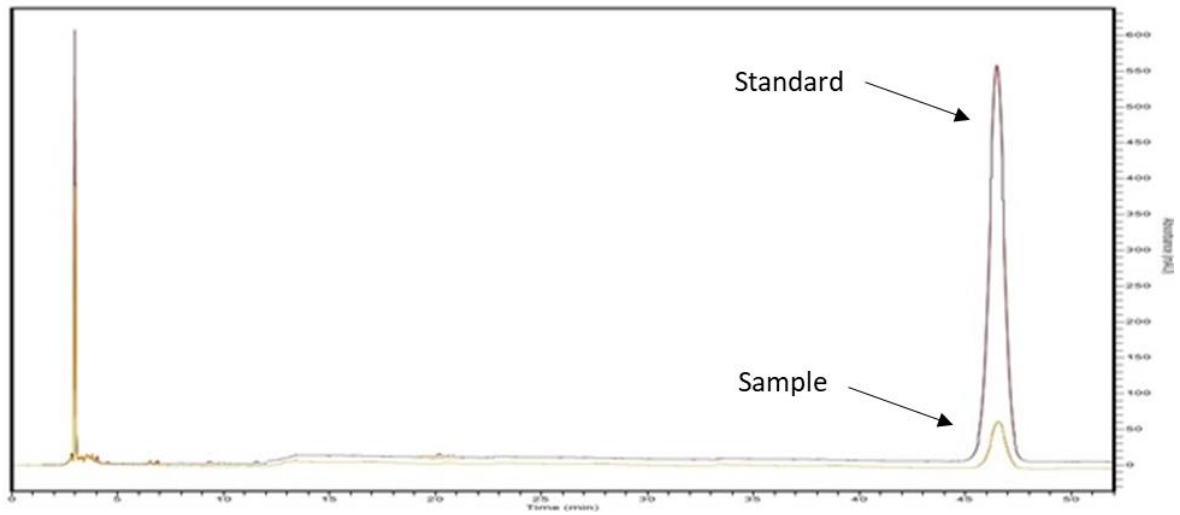

Figure 5: HPLC chromatogram for the analysis of squalene.

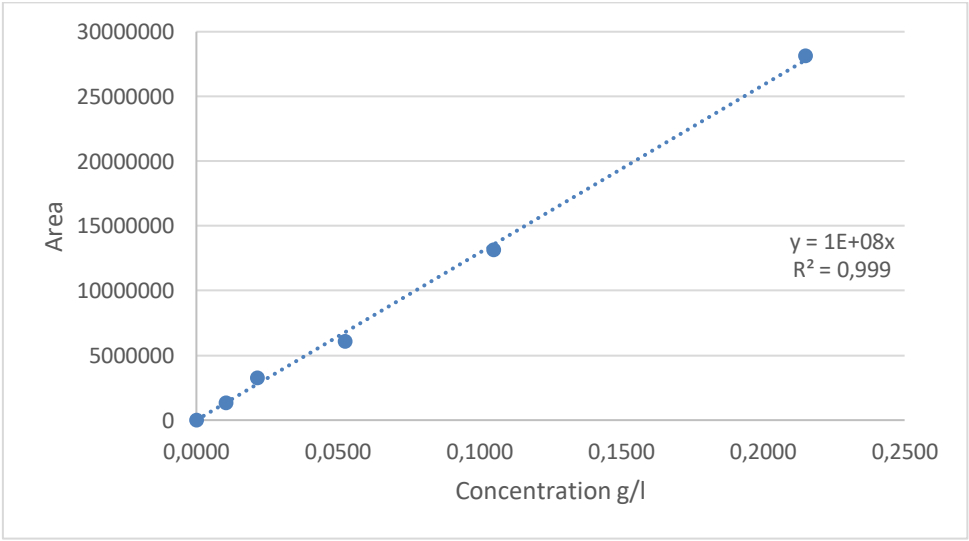

Figure 6: Squalene calibration curve

3.3 Results and discussion.

The research activity on *Amaranthus cruentus* seeds followed a classical univariate approach and was finalized to optimize the parameters of the SC-CO_2 based extraction process able to give the highest yield in oil with the highest content in squalene from *Amaranthus cruentus* seeds as raw material.

According to the classical univariate approach, a preliminary series of SC-CO_2 extraction tests were performed maintaining a constant process temperature of 40°C and testing three levels of extraction pressures: 300, 350 and 400 bars. These processes parameters were identified based on prior knowledge from Exenia. These tests also allowed us to obtain oil samples that were studied to claim the extraction of the biological active squalene. In figure 5 are compared the chromatograms of squalene standard and a squalene containing oil sample. Perfect correspondence of elution profile and of elution times is observable. The quantities of oil extracted in this first set of experiments are reported in table 2 and in figure 7. The pressure of 350 bars has been identified as optimal; the increasing of the pressure to 400 bars didn't give a significantly good result.

Table 2. List of the experiment run to explore the response "Yield in oil".

Pressure (bar)	Temperature (T°C)	Yield in oil (g)
300	50	11,0
300	50	12,4
300	50	13,0
350	50	62,0
350	50	55,9
350	50	58,0
400	50	60,0
400	50	64,0
400	50	62,0
350	40	50,1
350	40	52,4
350	40	48,0
350	50	65,0
350	50	92,0
350	50	85,0
350	60	85,0
350	60	100,2

350	60	90,0
350	70	96,4
350	70	94,0
350	70	95,0

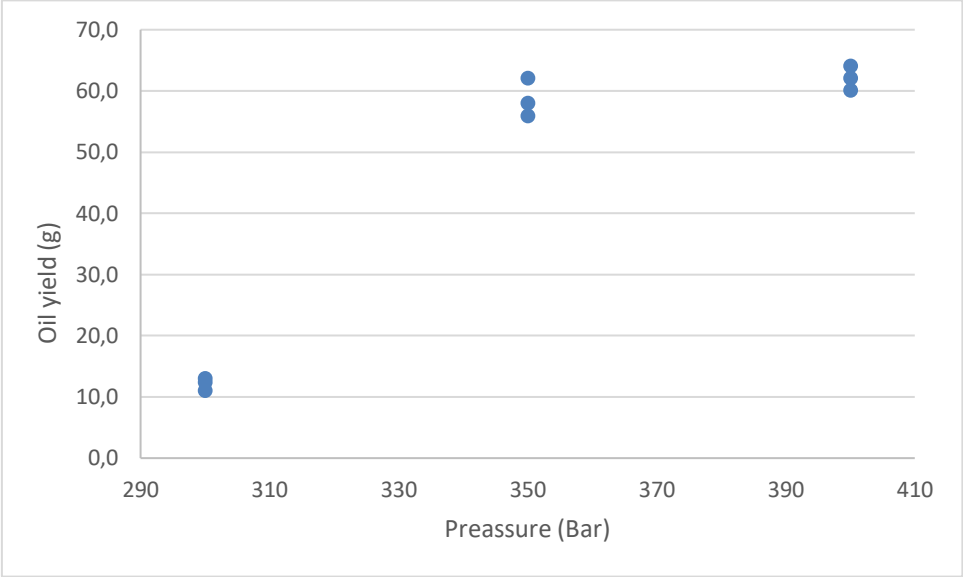

Figure 7. Plot of response yield in oil vs pressure.

A second series of experiments have been run fixing the pressure at 350 bars, based on previous tests, exploring four different temperatures: 40, 50, 60 and 70°C.

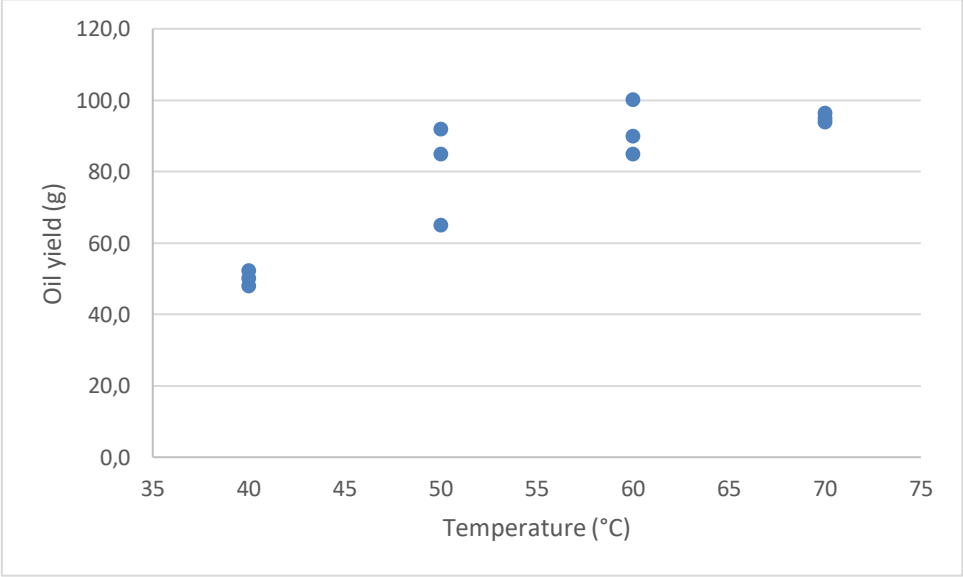

Figure 8. Plot of response yield in oil vs temperature

Again, the responses taken into consideration were the weights of extracted oil that were reported in figure 8 and table 2 vs temperature. The best compromise between the yield in oil and energy consumption for heating is 50°C.

Using the best conditions previously identified (350 bars and 50°C), a last test, sampling every 45 minutes, was run to understand the best extraction time to obtain the highest concentration in squalene. In this case the percentage of squalene in oil fraction has been considered to find out the best extraction time. As it is possible to see in the figure 9 and from the data reported in table 3, the oil collected in the first 120 minutes contains the most percentage of the squalene, while the last fractions are less reach in squalene.

Table 3. Experiment run at fixed pressure and temperature, collecting all extract from the separator every 45 minutes.

Time (min)	Percentage of Squalene %	Extracted oil (g)
45	12,5	6,0
90	15,2	29,0
135	14,3	23,0
180	5,3	24,5
225	3,3	20,0
270	5,5	3,0

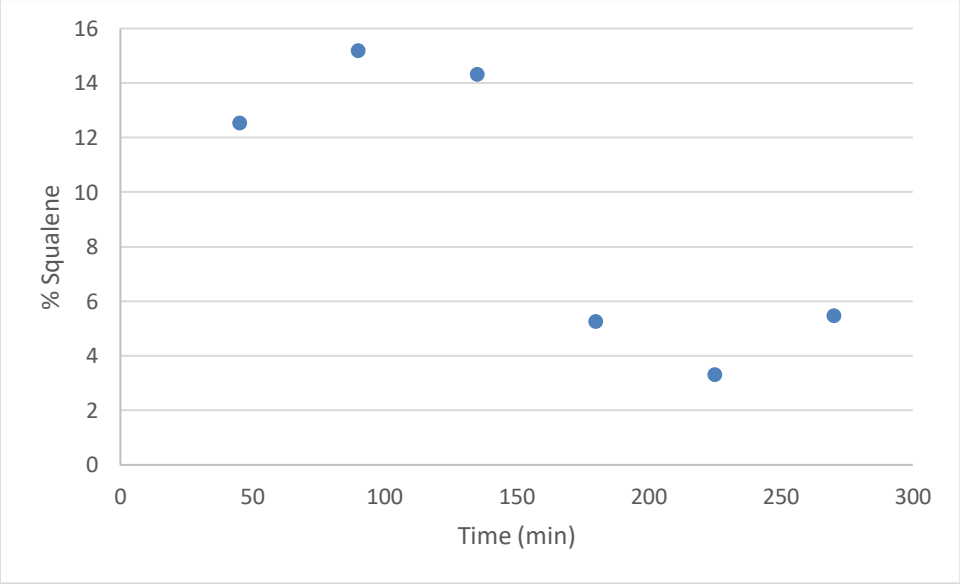

Figure 9. Plot of % of squalene vs time at 350 bars and 50 °C.

In the first year of this PhD, the classical univariate approach was applied to the experimental activity to explore the parameters of the SC-CO_2 based extraction process to improve the yield in oil with the highest content in squalene from *Amaranthus cruentus* seeds as raw material. 22 experiments were necessary to obtain an oil rich in squalene minimizing the process costs. The first 9 experiments explored the effect of pressure variable on the yield in weight of oil. The second group of 12 experiments, explored the role of temperature at the previously identified pressure value. With these 21 experiments the results seemed to be satisfying, so the percentage of squalene in the oil was evaluated every 45 minutes of extraction at 350 bars and 50°C. This last experiment allowed the understanding that the fraction of oil collected in the first 120 minutes is richer in squalene, while the second fraction had less content of this molecule. However, while having a low content in squalene, this second fraction was still interesting due to the nature of the oil and it's suitability for use in the cosmetic and food sectors. The results obtained thanks to the SC-CO_2 extraction (average yield in oil 6,5%) are comparable with results obtained with conventional solvents, as hexane, in Soxhlet extraction where the yield in oil is around 7,5% (Micera, 2021). Other research show how different Amaranth species present a comparable yield in oil, like the results presented by Krulj et Al., 2015. In this research the yield in oil and even the content of squalene can be compared to the result obtained in the present research work. However, this PhD research, underlined that, from an economic point of view it is interesting to split the extraction in two steps. In this way has been possible to obtain two different products that may have different price on the market.

Chapter 4. Tomatoes.

Introduction. In the second year of Doctorate the research moved to the valorisation of food waste material from the tomato paste production. One of the main problems of the food industry is the production of waste, which frequently includes a significant quantity of bioactive compounds (Ravindran & Jaiswal, 2016). Taking in to account this evidence, the focus of the present work was to make the best out of industrial tomato waste through supercritical carbon dioxide extraction. (Ashraf et al., 2020; Cadoni, Giorgi, Medda & Poma, 2000; Machmudah et al., 2012; Popescu et al., 2022; Romano et al., 2020; Vallecilla-Yepez & Ciftici, 2018). The industrial waste is mainly composed of tomato skins and seeds and can reach up to between 10 to 30 % of the initial weight of the fresh tomatoes (Savatovic, Cetkovic, Canadanovic-Brunet & Djlas, 2012). The content of bioactive compounds is quite varied where the main components are carotenoids, in which the most abundant is Lycopene. It is worth mentioning that industrial waste can be characterized by different chemical-physical features that could lead to different extracting outcomes and therefore the preliminary characterization step could be crucial.

Lycopene, a C40 polyisoprenoid compound containing 13 double bonds, is the most abundant carotenoid of the total pigment content of ripe tomatoes, and it was found to be a more efficient antioxidant than β-carotene, α-carotene, and α-tocopherol (Mascio, Kaiser & Sies, 1989; Rizk, El-Kady & El-Bialy, 2014). Recently, the regular consumption of foods rich in lycopene is arousing increasing interest, given the effects associated with the prevention of chronic cardiovascular diseases, protection against age-related macular diseases and several types of cancer (Costa-Rodrigues, Pinho & Monteiro, 2018).

Despite these interesting biological properties lycopene presents instability; with a view to protect it, as reported by Li, Cui and Hu (2023), encapsulation is an appropriate methodology to reduce degradation and control the release of lycopene, improve their bioavailability by affecting bio-accessibility. Led by this necessity, the encapsulation in nanoparticles lipidic carriers (NLCs) described in chapter 5 of this thesis has been tried.

Eventually, an appropriate comparison of the results between this present study and the various studies reported in the literature is necessary, but not straightforward for many reasons. Previous studies on similar materials (Choudhari, Ananthanarayan,

2007; Kumcuoglu, Yilmaz, Tavman, 2014; Ollanketo, Hartonen, Riekkola, Holm, Hiltunen, 2001) show results of decent Lycopene yield in oleoresin only on a laboratory scale (from about 5 g of starting material) and through different extraction methodologies like classic organic solvents extraction, ultrasound or microwave assisted technique and supercritical CO_2 extraction, but none of them on an industrial scale. Furthermore, the aforementioned studies tended to run the extractions using whole tomatoes, or peels, or seeds. Only few of them used waste materials and, in particular, industrial waste like the one assessed in the present work. To make matters worse, the comparison of results in terms of yields, particularly in lycopene, are expressed in many diverse ways which vary from paper to paper.
The choice made to carry out this project was guided by the interests of Exenia who outlined the research.

4.1 Materials.

Tomato seeds and skins were provided in dried form (content of moisture lower that 5% (v/v)) by Bio Agricola Fratelli Solarino A.a.s.s.a. based in Rosolini (SR) - Italy as waste material resulting from industrial tomato sauce production. Two different types of waste were considered: waste coming from tomatoes harvested in early spring, and a waste coming from summer harvested tomatoes. Food grade carbon dioxide was obtained by Nippon Gases S.r.l., HPLC grade solvents (tetrahydrofuran, methanol, acetonitrile) and standard lycopene were supplied by Merck KGaA.

4.2 Methods.

SC-CO_2 Extraction. The extraction has been performed using the same plant described previously in chapter 4 for the extraction of *Amaranthus cruenthus* oil. The quantity of dried tomato seeds and skins has been fixed at 600 gr. It has been used the 5L vessel volume extractor, and extract has been collected from the first gravimetric separator. Minimal and uninteresting material was collected from the two cyclonic separators. To optimize lycopene extraction a multivariate approach was applied in order to evaluate the role of temperature, pressure, flow, harvesting period of tomatoes (spring or summer). Replicates of experiments have been led by the design methodology.

HPLC analysis. The content of lycopene in oil was determined by HPLC analysis, with a quaternary Flexar pump, manual injection valve with a 20 µL loop, Perkin Elmer column oven, Perkin Elmer PDA Plus detector (Perkin Elmer), equipped with reverse phase C18 column (Alltima C18 250x4,6mm, 5µm), thermostated at 25°C, flow rate 1 ml/min and detection wavelength of 502 nm. As far as the eluent is concerned the literature suggests (Barba et al. 2006; Wimalasiri et al., 2017) to analyse lycopene by elution with a mixture of THF, methanol and acetonitrile. An experimental design has been applied to explore the elution time response surface to optimize the HPLC methodology for the quantitative determination of lycopene in extracts by SC-CO_2, considering in particular the separation from β-carotene peak.

The relevant variables have been shown to be the ratio between the solvents. Since the problem is about the proportion of solvent, and the total amount of solvents should always be 100%, the best methodology is a mixture design based on a ternary plot (Figure 10), in which each vertex is a pure substance, in our case a pure solvent: X1= THF; X2= Methanol; X3=Acetonitrile.

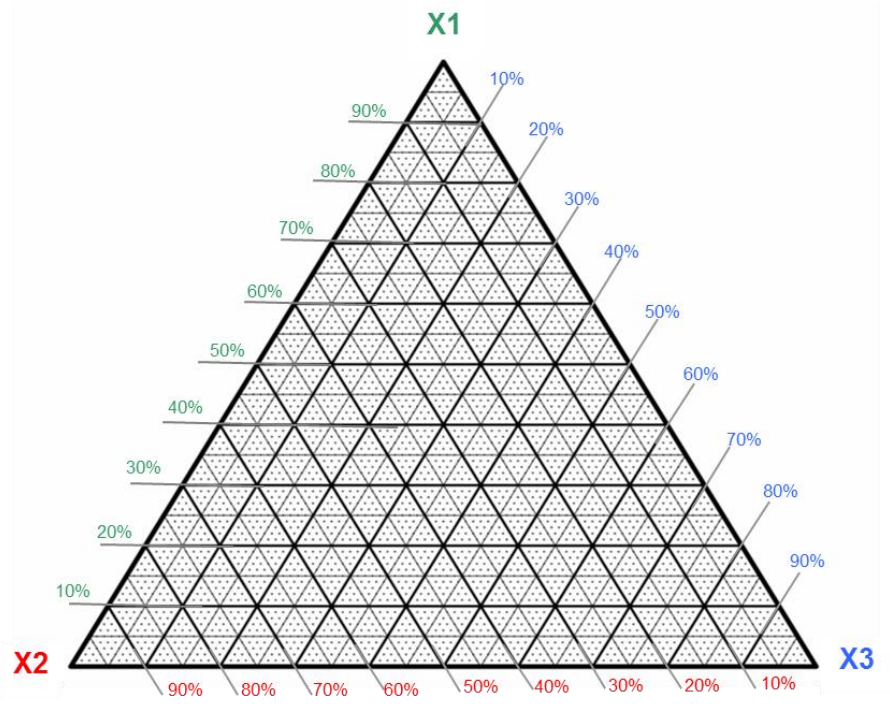

Figure 10. Ternary plot. X1= THF; X2= Methanol; X3=Acetonitrile.

However, an analysis made with 100% of a pure solvent wouldn't work, so it is important to work with principal component. A principal component is a specific point

in the ternary plot, which is composed by a mixture of the three solvents and is considered as a vertex for a new ternary plot. The principal components have been identified starting from a ternary composition that is already known to give discrete results but is not optimized for the specific matrix.

The design was developed around the values reported in literature (Wimalasiri et all., 2017), e.g. 55:25:20 THF:MeOH:ACN, that meet the solubility of lycopene. A first mixture design has been performed considering the following range:

- 55 % ≤ THF ≤ 45 %
- 35 % ≤ MeOH ≤ 25 %
- 30 % ≤ ACN ≤ 20 %

Table 4 lists the experimental plan and matrix with results. The experiments have been run in random order. As it is possible to see, the experiment which has the highest elution time is the experiment number 2 in table 4. The figure 11 shows a graphic representation of the results; in particular, each vertex of the triangle is a principal component (the first three experiments of table 4).

Table 4. List of the run experiments and relative results.

exp	Coded			Actual (%)			Response
	THF	MeOH	ACN	THF	MeOH	ACN	(min)
1	1,00	0,00	0,00	55	25	20	3,06
2	0,00	1,00	0,00	45	35	20	3,68
3	0,00	0,00	1,00	45	25	30	3,46
4	0,50	0,50	0,00	50	30	20	3,20
5	0,50	0,00	0,50	50	25	25	3,27
6	0,00	0,50	0,50	45	30	25	3,42
7	0,33	0,33	0,33	48,33	28,33	23,33	3,32

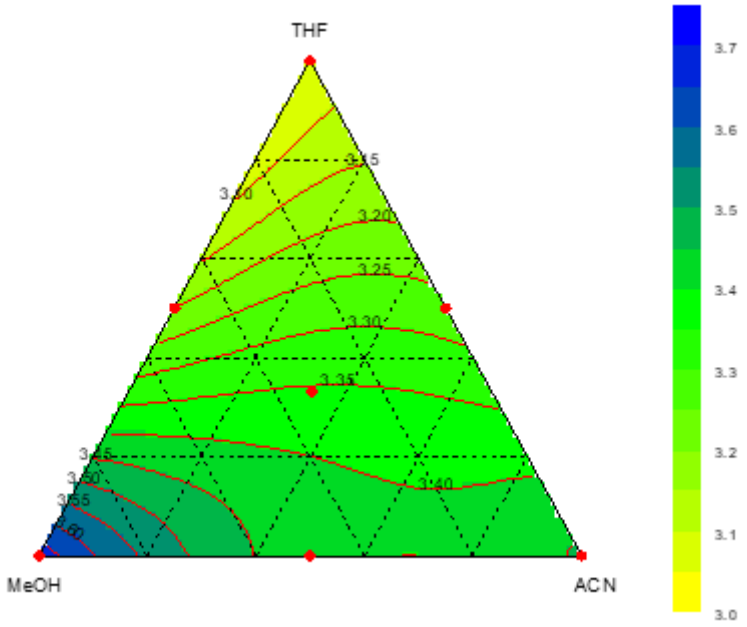

Figure 11. Response surface for the mixture design. Blue means a hight value for response, yellow a low value.

The yellow areas show the experiments with lower elution time, while the blues ones the experiments with highest elution time.

The result of the first design seems promising however the optimum doesn't fit with the expected separation of β-carotene and so an adequate analysis of lycopene. A second design was run, and the chosen starting point was the sweet point from the previous design which was developed around the following values:

51,7 % ≤ THF ≤ 41,7 %, 41,7 % ≤ MeOH ≤ 31,7 %, 26,7 % ≤ ACN ≤ 16,7 %

Table 5. List of the experiments run and relative results.

exp	Coded			Actual (%)			Response
	THF	MeOH	ACN	THF	MeOH	ACN	(min)
1	1,00	0,00	0,00	55,0	30,0	15,0	3,012
2	0,00	1,00	0,00	40,0	45,0	15,0	3,803
3	0,00	0,00	1,00	40,0	30,0	30,0	3,965
4	0,50	0,50	0,00	47,5	37,5	15,0	3,347
5	0,50	0,00	0,50	47,5	30,0	22,5	3,718
6	0,00	0,50	0,50	40,0	37,5	22,5	3,873
7	0,33	0,33	0,33	45,0	35,0	20,0	3,524

Table 5 lists the experimental plan and matrix with results. The experiments have been run in a random order.

The experiment that has the highest elution time is enumber 3. The figure 12 shows a graphic representation of the results, in particular each vertex of the triangle is a principal component (the first three experiments in table 5).

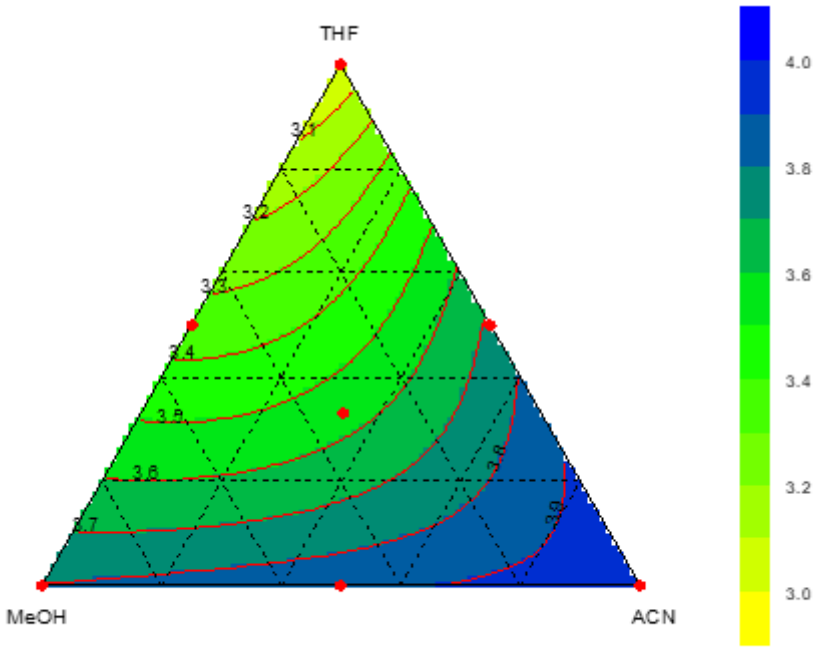

Figure 12. Response surface for the mixture design. Blue means a hight value for response, yellow a low value.

The yellow areas show the experiments with lower elution time, while the blue ones the experiments with highest elution time. The result fits the quality required for the analysis so the lycopene analysis have been conducted following a isocratic elution with a mixture THF:MeOH:ACN (40:30:30).

Two series of standard solution have been prepared dissolving respectively 0,0028 gr of standard lycopene in 100 ml THF and 0,0013 gr of standard lycopene in 10 ml THF and then both diluted 1:2 in a solution 50:50 Acetonitrile:MeOH. Before injection in the column the solutions have been filtered on a syringe filter in PTFE D.25 mm, 0,45 µm. With the purpose to obtain a calibration curve, a series of other dilutions have been performed to obtain a lycopene concentration range between 0,028 and 0,13 g/L. Lycopene peak area has been plotted vs concentration to obtain a calibration curve ($y= 3*10^7 x$; $R^2=0.9995$) reported in figure 13.

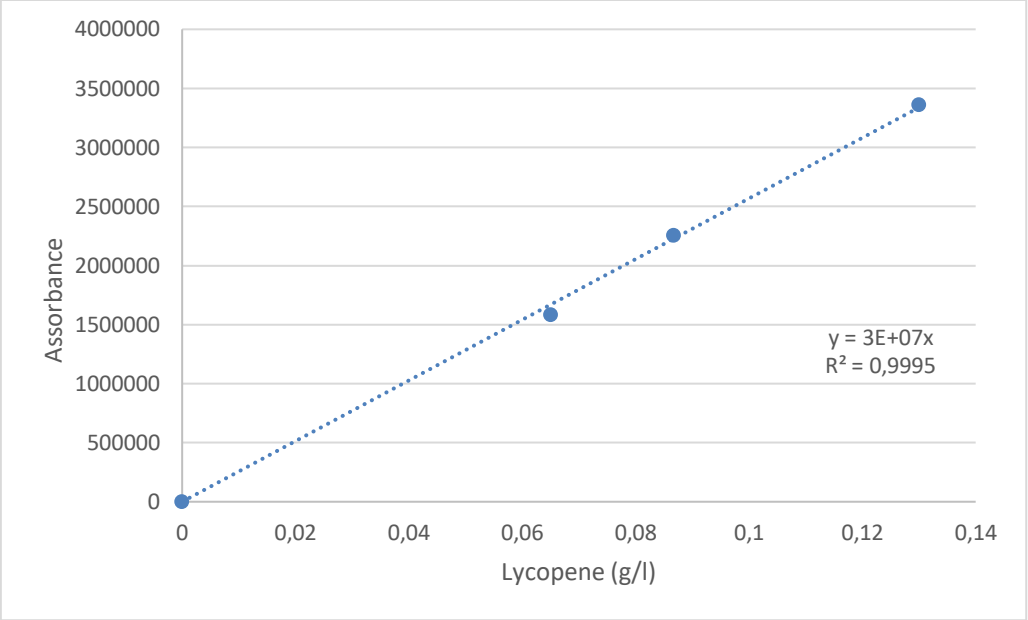

Figure 13. Lycopene calibration curve.

In figure 14 the chromatograms of lycopene standard and oil extracted in experiment number 12 (table 7) taken as an example. Perfect correspondence of elution times is observable. The very small pick present at 3,5 minutes elution time is due to other carotenoids, in particular β-carotene.

Each sample of extracted oil has been prepared in the same way as the standard solution: 0,1 gr is dissolved in 10 ml of THF and then diluted 1:2 with a solution 50:50 ACN:MeOH.

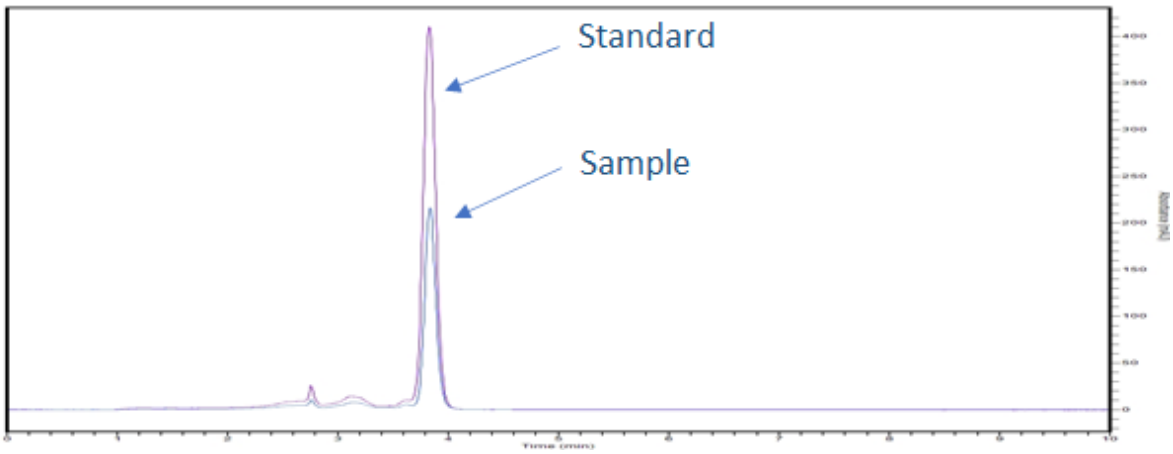

Figure 14. HPLC chromatograph for the analysis of lycopene.

If necessary, the samples are further diluted to fit the calibration curve concentration range. Before injecting it in the column the solution is filtered in a syringe filter in PTFE D.25 mm, 0,45 µm.

Experimental design. A multivariate approach has been applied to optimize the NLCs synthesis because the number of experimental variables that must be considered is 4. A classical univariate approach would have required 36 experiments to obtain the same information - a very heavy and time consuming experimental activity, mostly because of the lack of raw material.

According to the multivariate approach, table 6 lists the variables together with their respective levels. Process parameters such as pressure and temperature, respectively in the range 200-350 bar and 60-80 °C, were studied at three levels with the aim of studying a possible curvature in the response. Another important parameter is the contact time between SC-CO_2 and raw material in the extraction vessel and therefore the SC-CO_2 flow was considered and studied in a reasonable range (18-24 kg/h) assessing two levels only. Together with the process parameters, two batches of tomato waste characterized by a different harvesting times (spring and summer harvest) were considered. The extraction time was kept constant (3 hours) as well as the amount of tomato waste useful for the extraction (600 g).

Table 6. List of variables with relative levels that have been identify as relevant to the system.

		Levels		
VAR ID	**Variable Name**	**-1**	**0**	**1**
$\mathbf{X_1}$	Pression (bar)	200	275	350
$\mathbf{X_2}$	Temperature (°C)	60	70	80
$\mathbf{X_3}$	Flow (Kg/h)	18		24
$\mathbf{X_4}$	Batch	A (early harvest time)		B (late harvest time)

To study the effect of the above-mentioned variables, the experimental plan was chosen according to the experimental design (DoE) approach. Following this method, it is possible to obtain a higher quality of information that can be obtained starting from a reduced experimental effort. In this case, the experimental effort is the most critical aspect, due to the very limited availability of raw material (industrial tomato waste with two different quality characteristics).

According to the number of the variables and their respective levels, the postulated multiple linear regression model is composed of 13 coefficients: 1 constant, 4 linear terms, 6 interactions, 2 quadratic terms for pressure and temperature variables:

$Y = b_0 + b_1X_1 + b_2X_2 + b_3X_3 + b_4X_4 + b_{12}X_1X_2 + b_{13}X_1X_3 + b_{14}X_1X_4 + b_{23}X_2X_3 + b_{24}X_2X_4 + b_{34}X_3X_4 + b_{11}X_1^2 + b_{22}X_2^2$

Y = response

b_0 = constant

b_1 = linear term (pressure)

b_2 = linear term (temperature)

b_3 = linear term (flow)

b_4 = linear term (tomato batch)

b_{12} = interaction (pressure-temperature)

b_{13} = interaction (pressure-flow)

b_{14} = interaction (pressure-tomato batch)

b_{23} = interaction (temperature-flow)

b_{24} = interaction (temperature-tomato batch)

b_{34} = interaction (flow-tomato batch)

b_{11} = quadratic term (pressure)

b_{22} = quadratic term (temperature)

To estimate both linear and quadratic terms at different levels it was not possible to use traditional designs, therefore the D-optimal design was selected.

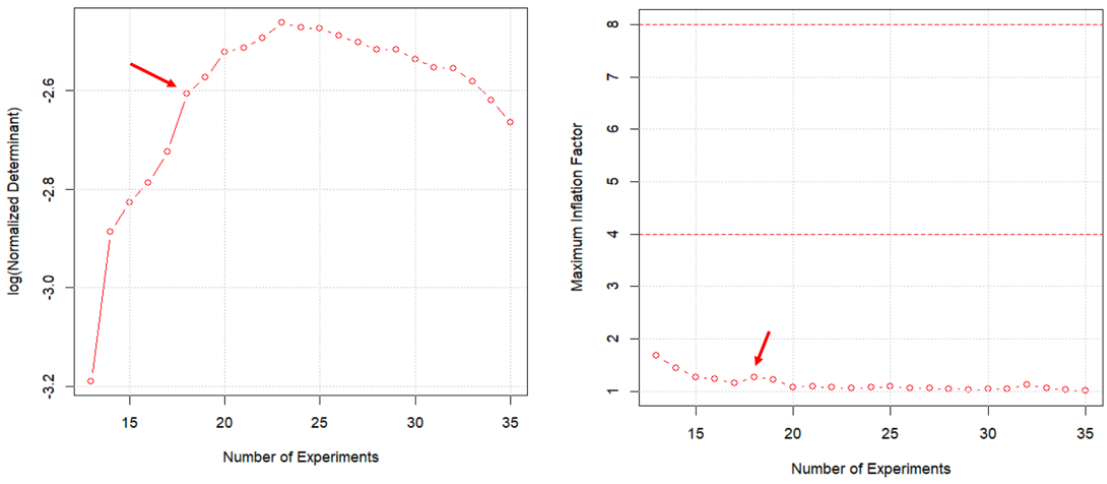

Figure 15. Normalized determinant (left) and inflation factor (right) chart; Each chart has number of experiments on x axis; Normalized determinant has log (normalize determinant) on x axis, while inflation factor has maximum inflation factor value.

The D-Optimal design is useful to find the best compromise between the information and the possible experimental effort (Leardi, 2009; Leardi, 2018).
According to the normalized determinant and the inflation factors, a sub-optimal solution of 18 experiments, from a total of 36 possible combinations (3^2*2^2), was selected (Figure 15).

This number was selected due to the very limited availability of the different types of tomato waste. For the same reason, only four replicates were selected to evaluate the experimental variability. The replicates were selected through the D-optimal Design by addition strategy, useful to select the best informative condition within the proposed experimental matrix.

Four experiments out of twenty-two gave odd experimental results: three of them were repeated and included in the model (replicates 5, 6, 7). Only experiment 7 (experimental condition: 200 bar, 60 °C, 24 Kg/h, batch B) could not be repeated due to the lack of tomato waste characterized by summer harvest time (batch B).

Finally, 24 experiments were available to estimate 13 coefficients, with 11 degrees of freedom. Table 7 lists the experimental matrix and plan, obtained by randomizing the experiments order. The data analysis was performed through CAT (Chemometric Agile Tool) software (Leardi, Melzi, Polotti).

Table 7. List of the experiments performed.

Exp	Coded values				Actual values				Responses		
	Pressure (bar)	Temperature (°C)	Flow (Kg/h)	Batch	Pressure (bar)	Temperature (°C)	Flow (Kg/h)	Batch	Oil (g)	Lycopene (mg/g)	Replicates
1	1	1	1	1	350	80	24	B	26,11	136,2	
2	1	-1	1	-1	350	60	24	A	16,69	26,2	r1
3	0	1	-1	1	275	80	18	B	17,62	292,7	r2
4	-1	-1	1	-1	200	60	24	A	12,4	20,4	r3
5	1	0	-1	1	350	70	18	B	20,03	149,3	
6	-1	0	-1	1	200	70	18	B	10,09	134,3	r4
7	-1	-1	1	1	200	60	24	B			
8	1	-1	-1	-1	350	60	18	A	13,46	69	
9	-1	-1	1	-1	200	60	24	A	12,55	40,1	r3
10	-1	1	1	-1	200	80	24	A	9,42	91,4	
11	0	-1	-1	1	275	60	18	B	12,91	12,9	
12	0	1	-1	1	275	80	18	B	18,98	10,9	r2

13	-1	-1	-1	-1	200	60	18	A	13,24	18,9	r5
14	0	0	-1	-1	275	70	18	A	10,23	60,8	
15	-1	1	-1	-1	200	80	18	A	5,13	65,3	r6
16	0	0	1	1	275	70	24	B	17,43	232,8	
17	-1	1	1	1	200	80	24	B	14,31	72,9	
18	1	1	1	-1	350	80	24	A	11,93	205,7	r7
19	1	1	-1	-1	350	80	18	A	6,86	11,7	
20	-1	-1	1	1	200	60	24	B	14,97	267,2	
21	-1	0	-1	1	200	70	18	B	14,12	453,4	r4
22	-1	-1	-1	-1	200	60	18	A	8,97	51,9	r5
23	1	1	1	-1	350	80	24	A	19,38	279,8	r7
24	-1	1	-1	-1	200	80	18	A	4,88	60.0	r6
25	1	-1	1	-1	350	60	24	A	13,54	30,1	r1

4.3 Results and discussion.

After running all the experiments and collecting the results, a multiple linear regression (MLR) was carried out. Stars represent the statistical significance (p-value; * = 0.05, ** = 0.01, *** = 0.001).

Oil (g) = 14.15 + 2.85X1(**) + 0.08X2 + 1.55X3(*) + 3.03X4(**) + 0.89X1X2 + 0.41X1X3 + 1.12X1X4 + 0.53X2X3 + 1.77X2X4 (*) - 0.32X3X4 + 0.01X12 + 0.12X22

Residual standard deviation: 2.63 (11 degrees of freedom); % explained variance: 71.93.

The experimental variability was assessed through a pooled standard deviation, which gave an acceptable result of 2.70, estimated with 7 degrees of freedom. Since the residual standard deviation and the experimental standard deviation were not significantly different, there is no lack of fit. The linear terms for pressure (X_1), flow (X_3) and batch kind (X_4) variables are significant (both X_1 and X_4 at $p<0.01$; X_3 at $p<0.05$). The temperature-batch interaction (X_2X_4) is also significant ($p<0.05$). The linear terms show that a better response is achieved at higher pressures and higher flows (Figure 16). The better response at higher pressure could be due to major increase of solvent viscosity that promote the affinity with higher molecular weight compounds. The better response correlated to the highest flow could be justified by the higher mechanical thrust that improves the mass transfer from the matrix to the solvent.

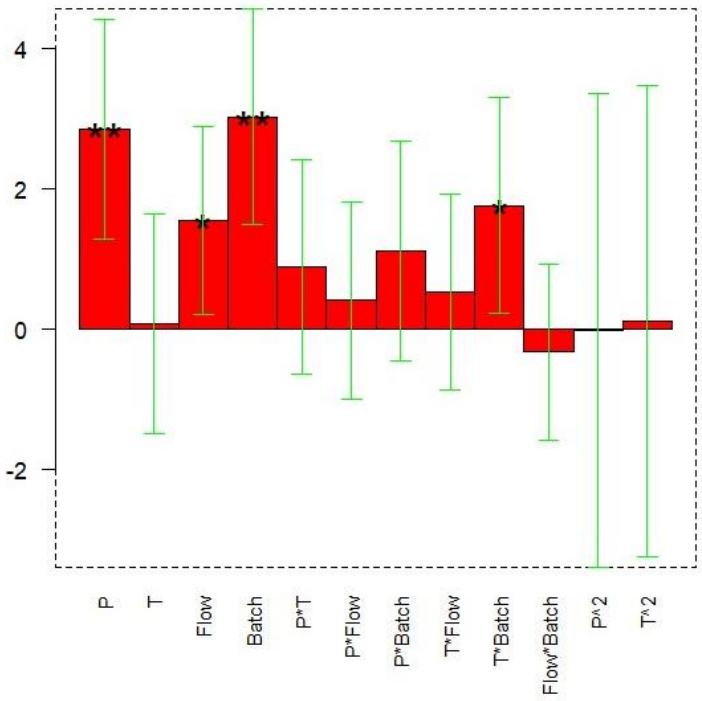

Figure 16. Coefficents for Oil response.

To interpret the batch effect and the interaction that occurs between temperature and batch variables, the response surface was analysed (Figure 17). The response surface is shown in the plane temperature-batch (X_2-X_4) by setting the pressure (X_1) and flow rate (X_3) variables both at their best extraction conditions (both at level +1; respectively at 350 bar and at 24 kg/h). To visualize the uncertainty associated with the response, the semi-amplitude of the confidence interval is shown (Figure 17). By observing Figure 17, it is possible to interpret the interaction: the effect of temperature is present only in batch B (level +1; summer harvest) where higher temperatures lead to a greater quantity of extracted oil, while in batch A (level -1; spring harvest) this effect is completely absent. In this case, higher temperatures work better in batch B than batch A, therefore it can be a synergy between temperature and degree of ripeness, where higher temperatures seem to work better at a higher degree of ripeness. With batches characterized by a lower degree of ripeness, however, it could be possible to work with more conservative operating conditions characterized by a lower temperature, saving production costs. This evidence also leads to another logical conclusion: it is important to characterize the starting material because the best process parameters could change based on its characteristics.

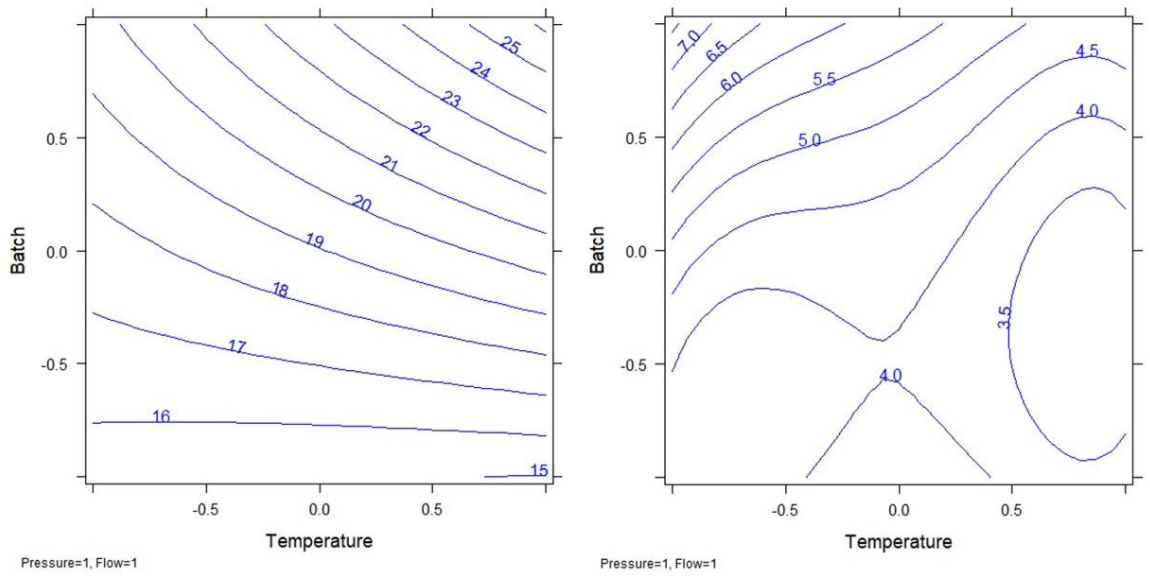

Figure 17. Contour plot (left) and semi amplitude (right) of the confident interval for the interaction Temperature/Batch.

Regarding the Lycopene response, the concentration values showed a great experimental variability and therefore it is necessary to consider further studies on the analytical method before computing any model. It has not yet been clarified whether the variability derives from experimental conditions in extraction or from the analytical technique. It can reasonably be assumed that an error in the analysis is due to the instability of the molecule in the chosen solvent. Further studies will clarify this point and allow to perform and analysis of the Lycopene response.

Thanks to the experimental design it was possible to find the best conditions for extracting oil containing lycopene from tomato waste by exploring the entire experimental domain. Furthermore, the experimental design showed that the analytical method used to quantify lycopene needs to be improved since the experimental variability nearly covers the imposed variability. All the factors assessed were significant, where the greatest effects on the oil extraction were related to pressure and tomato batch, followed by flow. To increase the response, it is important to work with both pressure and flow at the highest level. The temperature increase was only important when considering the summer harvested tomato batch, whereas the extraction process can operate even at the lowest temperature (in the range considered) on the batch harvested in early spring. For future extractions, other characteristics of the starting material will also be evaluated to better understand the

phenomenon and therefore identify other possible interactions with the process variables. In conclusion it is possible to say that the best extraction yield has been reached with the highest pressure explored (350 bars), the highest flow (24 kg/h), and with the tomato waste harvested in summer; temperature has no effect so it can be set at minimum explored value (60°C). However, if only the waste resulting from tomato waste coming from a spring harvest is available, it is possible to maximize the extraction yield working with the same conditions as previously mentioned but setting the temperature at maximum explored value (80°C).

The oil extracted using this optimization process will be further analysed to determine its antioxidant activity. Hopefully, the synergic effect of lycopene and minor carotenoids present in the oil will allow high antioxidant activity levels. The importance of lycopene and its antioxidant activity in diet is related to the prevention of chronic cardiovascular diseases, protection against age-related macular diseases and several types of cancer. However, carotenoids are well known to be unstable compounds, for this reason the next challenge will be the synthesis of a nanostructured lipid carrier that preserves the antioxidant activity of the lycopene rich oil obtained in the present work.

Chapter 5. Lycopene based NLCs

Introduction. After the optimization of the extraction process, in collaboration with university Sorbonne Paris Nord, the following period of work was characterized by activity regarding the antioxidant and encapsulating the extract in order to stabilize it and make it suitable for further use.

For the further experiments a mix of all the extracted material obtained by previous extraction tests were gathered in order to have enough to run all the tests. All the samples were defrosted and melted at room temperature. After the melting process all the samples were poured into a beaker and homogenized well by continuous stirring and mixing from bottom to top. This extract has been frozen in an amber glass jar.

The lycopene, the bioactive molecule present in Exenia oleoresin, has 13 double bonds, 11 of which are conjugated, and is responsible for the scavenging reactive oxygen species (ROS), in particular the singlet oxygen ($^1O_2$). This structure allows lycopene to be one of the most potent antioxidants among the carotenoids (Jia, 2020). However, the very same structure that allows lycopene to be such a powerful bioactive is also responsible for its instability. Indeed, the high number of conjugated double bonds is responsible for its susceptibility to isomerisation and oxidation during processing, in the presence of oxidants, light, and temperature (Souza et al., 2018). The common isomer of lycopene in nature is the more stable trans configuration; however, going through processing and storage, lycopene can easily rearrange in cis isomer or oxidize, with the consequent decrease or loss of the colorant power and biological properties (Nunes et al., 2007). As reported by Li, Cui and Hu (2023), encapsulation is an appropriate methodology to reduce degradation and control the release of lycopene, improve their bioavailability by affecting bio-accessibility. For this reason, the research done during the third year of Doctorate was focused on the synthesis of nanoparticles lipidic carriers (NLCs), with the purpose of protect lycopene. In literature, similar nanoparticles have been obtained with an average yield in encapsulation percentage of 51% by spry drying process (Nunes, and Mercadante, 2007) meanwhile freeze-dry methodology gives back a higher value, close to 84% of encapsulation (Souza, et al., 2018). Several methodologies, like traditional emulsion, microcapsule, solid lipid nanoparticles etc., can be applied in other to obtain this result, and each of them have different advantages and disadvantages (Li, Cui and Hu, 2023).

Among all the methodologies, to reach the goal of protect Lycopene antioxidant activity in this research project, one of the best consolidated methodologies by the INSERM U1148, Laboratory for Vascular Translational Science, Cardiovascular Bioengineering, Villetaneuse, France was chosen and followed. This procedure has already been used to perform NLCs synthesis to protect the antioxidant activity of other interesting antioxidants like Astaxanthin (Rodriguez-Ruiz et Al. 2018) or Curcumin (Calderon-Jacinto et Al 2022).

To perform the synthesis of NLCs several components are needed, such as lipids, surfactant both for lipid and water phase. In the present work substances that may be accepted by cosmetics and pharmaceutical industry were chosen.

5.1 Materials.

The encapsulation tests were performed on a mixture of all the extracted oils obtained by SC-CO_2 extraction test, hereinafter referred to simply as oleoresin, so as to have enough material to run all the experiments. All the samples were defrosted at room temperature and homogenized well in a beaker by continuous stirring and mixing bottom to top. The oleoresin have been frozen in an amber glass jar. The content of lycopene in oleoresin was extimated to be 0,5 %. Standard lycopene, ammonium salt of acid 2,2'-azino-bis(3-ethilbenzothiazoline-6-sulphonic), potassium persulfate, stearic acid and all solvents were supplied by Merck KGaA. Compritol was provided by Gattefossé. PHOSAL® 50 SA+ (Phospholipid formulation with >50% of Phosphatidylcholine), PHOSAL® 75 SA (Phospholipid formulation with >72% of Phosphatidylcholine) were provided by Lypoid GmbH.

5.2 Methods.

Determination of lycopene content in oleoresin. The lycopene content of the oleoresin samples has been evaluated next the laboratory of Sorbonne Paris Nord University by a spectrophotometric procedure. 0,2 g of oleoresin have been dissolved in 10 ml of chloroform, and after several dilutions (from 1:10 to 1:50) in chloroform to obtain different concentrations (at least three replications for each concentration) the absorbance spectra was recorded with a Safas-Monaco spectrophotometer at 483nm and compared with a calibration curve carried out solubilising lycopene standard in chloroform with a concentration range between 0,9 and 18,6 µM ($y=0,0684x$; $R^2=$

0,9989). The lycopene content from the oleoresin samples are expressed as lycopene percentage on the extract. The diluted solutions were stored in the dark and at 4°C until the next day and the absorbance readings were repeated. The same values of the previous day were obtained to confirm the stability of the lycopene under the experimental conditions.

Evaluation of antioxidant activity. The antioxidant activity of the oleoresin and NLCs samples were evaluated by α-TEAC assay, a lipophilic modified test inspired by the initial TEAC assay of Miller et al (Arts et al., 2004). The test is based on the reaction of a solution 17 mM in distilled water of diammonium salt of ABTS (2,2'-azino-bis(3-ethylbenzothiazoline-6-sulfonic acid)) with a strong oxidant ($K_2S_2O_8$) in solution 1,9 mM in distilled water, ratio 1:1 v/v, to obtain the radical cation of ABTS ($ABTS^{*+}$) that shows a characteristic blue colour with an absorption at 734 nm that is quenched in presence of a product with antioxidant properties.

A stock solution of $ABTS^{*+}$ is prepared as follows reported. Two solutions were prepared by dissolving 40 mg of diammonium salt of ABTS in 5 ml of distilled water and 13,6 mg of $K_2S_2O_8$ in 10 ml of distilled water respectively. 0,5 ml of each solution were mixed and stored in cool and dark place for 12 hours and then diluted 1:70 v/v with distilled water to reach an absorbance of about 0,8. 1000 µl of this $ABTS^{*+}$ stock solution was mixed with 300 µl of molecule of interest solution prepared as described below. The test was performed for α-tocopherol, as a standard inhibition reference, with five solutions within a content of α-tocopherol between 20µM and 100µM in chloroform. For each concentration three replicants were performed. For oleoresin, the test was run with eight solutions within 5µM and 40µM of lycopene in chloroform. For each concentration three replicants were performed. While running the test on NLCs, a pre-treatment was performed. 1ml of suspension of NLCs were centrifuged for 30 minutes at 13.000 rpm. The supernatant was collected and diluted 1:4 in a mixture methanol: dichloromethane (60:40) and shacked in a vortex mixer. This solution was used for further measurements since with this procedure it is mandatory to open the NLCs and consider the inside oleoresin for tests. Within this solution, five solutions were prepared with a content of lycopene between 2,5µM and 40,8µM. The same test was run with the standard lycopene dissolved in chloroform. Six solutions were

prepared with a concentration between 5mM and 40mM. For each concentration three replicants were performed.

To apply equation 1, it was also necessary to have the absorbance value without any antioxidant molecule, measured on a solution prepared adding 300 µl of the solvent used to solubilize the molecule of interest (chloroform for α-tocopherol and oleoresin, methanol:dichloromethane mixture (60:40) for NLCs) to 1000 µl $ABTS^{*+}$ stock solution. After being protected from light, 60 minutes shaking and centrifugation 5 minutes, the absorbance of the aqueous phase is measured at 734 nm and compared with the absorbance of stock solution. The inhibition percentage for sample at each concentration is calculated applying equation 1.

$$\%\ of\ inibition = \frac{Absorbance\ of\ ABTS{\cdot}+\ stock\ solution - Absorbance\ of\ interest\ molecule}{Absorbance\ of\ ABTS{\cdot}+\ stock\ solution} * 100 \qquad (1)$$

The inhibition curve for each sample was obtained by plotting the % of inhibition as function of the relative concentration. The α-TEAC value is the ratio between the slope of the inhibition curve for the test molecule and the slope of the inhibition curve for the α-tocopherol.

NLCs synthesis. Two different solutions were prepared and heated at 75°C: 1) 15 ml of water solution containing 450 mg of Poloxamer 407, also known as Pluronic F-127; 2) a lipid phase containing 450 mg of stearic acid or Compritol, 60 mg of PHOSAL®50 SA+ or PHOSAL® 75 SA and 100 mg of lycopene enriched oleoresin. The lipid phase was mixed with a Polytron system at 10.000 rpm for two minutes; then, 2 ml of water Poloxamer 407 solution was added to the mixing oil phase and homogenized for two minutes raising the speed of the Polytron system up to 20.000 rpm. The remaining water solution was added and the system was kept mixed at 75°C for 30 minutes. Later, the pH was measured and set at 8 by adding small volume of a solution of NaOH 7,5M. The NLCs solutions were stored for at least one night at 4°C before analysis. The reported quantities for each component are relative to preliminary experiments run to evaluate the feasibility. For further experiments the quantity and type of products are given by the experiments referred in table 9.

Determination of lycopene content in NLCs. The determination of lycopene in NLCs required a pre-treatment. 1ml of suspension of NLCs were centrifuged for 30 minutes at 13.000 rpm to separate the excess of solid lipid as bottom phase (figure 18). The supernatant was collected and diluted 1:4 in a mixture methanol: dichloromethane (60:40) and shaken in a vortex mixer to open the NLCs.

Figure 18. Top and bottom phases after centrifugation of NLCs suspension.

The entrapped lycopene in NLCs was estimated by a spectrophotometric method using a Safas Spectrophotometer (Monaco). An additional calibration curve was obtained by solubilizing it in methanol:dichloromethane (60:40) mixture - a sample of oleoresin previously analysed in its lycopene content.

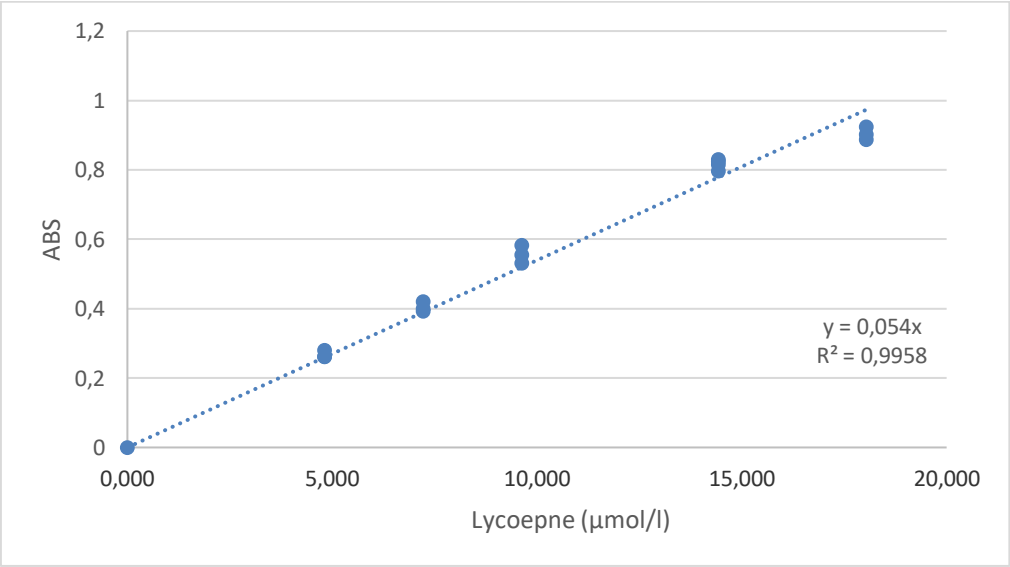

Figure 19. Calibration curve to extimate lycopene content in NLCs.

Absorbance has been measured at 473 and the absorbance was plotted vs concentration to obtain a calibration curve (figure 19) (y=0.054x); (R^2=0.9958). This procedure was necessary since the NLCs have been opened in a solution methanol:dichloromethane (60:40) while the calibration curve with standard lycopene was in chloroform. A dilution of the solution of opened NLCs in chloroform presents two main problems; the mixed solution is not limpid, and the dilution will over dilute the analyte so that it could no longer be revealed by the instrumentation.

The percentage of entrapped lycopene inside the NLCs was calculated by the equation 2.

$$\%\ of\ lycopene\ entrapped\ = \frac{Lycopene\ (\mu g)\ inside\ the\ NLCs}{Lycopene\ (\mu g)\ in\ the\ oleoresin\ used\ to\ prepare\ the\ NLCs} \quad (2)$$

DLS measurements. Particle size distribution and electrical potential at the slipping plane of the nanoparticles were determined using a Zetasizer Instrument. For particle side distribution the NLCs dispersed in water were centrifuged for 30 minutes at 13.000 rpm and after diluted 1:1000 in a PBS buffer solution, while for the measurement of electrical potential at the slipping plane the NLCs dispersed in water after centrifugation have been diluted 1:400 in a solution KCl 1μM.

Experimental design – D-optimal design. A multivariate approach was applied to optimize the NLCs synthesis because the the number of experimental variables that had to be considered was six. A classical univariate approach would have required 324 experiments to obtain the same information - a very time consuming experimental activity.

Table 8 lists the considered variables with relative levels. Above all the synthesis parameters, the one selected concerned the quantity and type of material used. The parameters identified as relevant to the synthesis are six. In particular, lipid chemical composition and surfactant chemical composition were studied, considering, Compritol or Stearic Acid and PHOSAL® 50 SA+ or PHOSAL® 75 respectively, at two levels. While another 4 parameters were considered at three levels, oleoresin quantity, lipid quantity, surfactant quantity and water phase quantity respectively between 100-300 mg, 350-450 mg, 60-120 mg, and 8-15 ml. The synthesis procedure previously explained was kept the same for each experiment.

Table 8. List of variables with relative levels that have been identify as relevant to the system.

		Levels		
VAR ID	Variable name	-1	0	1
X1	Oleoresin (mg)	100	200	300
X2	Chemical structure of Lipid	Compritol		Stearic acid
X3	Lipid (mg)	350	400	450
X4	Chemical structure of surfactant	PHOSAL® 50 SA+		PHOSAL® 75
X5	Surfactant (mg)	60	90	120
X6	Water phase (ml)	8	11	15

To study the effect of the above-mentioned variables, the experimental plan was chosen according to the experimental design (DoE) approach. Following this method, it was possible to obtain a higher quality of information that could be obtained starting from a reduced experimental effort.

According to the variables and their respective values listed in table 8, the postulated multilinear regression (MLR) model, including 26 coefficients (1 constant, 6 linear terms, 15 interactions and 4 quadratic terms) is as follows:

$$Y = b_0 + b_1X_1 + b_2X_2 + b_3X_3 + b_4X_4 + b_5X_5 + b_6X_6 + b_{12}X_1X_2 + b_{13}X_1X_3 + b_{14}X_1X_4 + b_{15}X_1X_5 + b_{16}X_1X_6 + b_{23}X_2X_3 + b_{24}X_2X_4 + b_{25}X_2X_5 + b_{26}X_2X_6 + b_{34}X_3X_4 + b_{35}X_3X_5 + b_{36}X_3X_6 + b_{45}X_4X_5 + b_{46}X_4X_6 + b_{56}X_5X_6 + b_{11}X_1^2 + b_{33}X_3^2 + b_{55}X_5^2 + b_{66}X_6^2$$

Y = response

b_0 = constant

b1 = linear term (oleoresin quantity)

b2 = linear term (chemical structure of lipid)

b3 = linear term (lipid quantity)

b4 = linear term (chemical structure of surfactant)

b5 = linear term (surfactant quantity)

b6 = linear term (water phase quantity)

b12 = interaction (oleoresin quantity- chemical structure of lipid)

b13 = interaction (oleoresin quantity- lipid quantity)

b14 = interaction (oleoresin quantity- chemical structure of surfactant)

b15 = interaction (oleoresin quantity- surfactant quantity)
b16 = interaction (oleoresin quantity- water phase quantity)
b23 = interaction (chemical structure of lipid- lipid quantity)
b24 = interaction (chemical structure of lipid- chemical structure of surfactant)
b25 = interaction (chemical structure of lipid- surfactant quantity)
b26 = interaction (chemical structure of lipid- water phase quantity)
b34 = interaction (lipid quantity - chemical structure of surfactant)
b35 = interaction (lipid quantity - surfactant quantity)
b36 = interaction (lipid quantity - water phase quantity)
b45 = interaction (chemical structure of surfactant - surfactant quantity)
b46 = interaction (chemical structure of surfactant - water phase quantity)
b56 = interaction (surfactant quantity - water phase quantity)
b11 = quadratic term (oleoresin quantity)
b33 = quadratic term (lipid quantity)
b55 = quadratic term (surfactant quantity)
b66 = quadratic term (water phase quantity)

Since both quantitative and qualitative variables at different levels were present, a D-optimal design was considered for the correct selection of the experiments instead of a traditional one, which was useful for finding the best compromise between the information and the experimental effort.

According to the normalized determinant and inflation factor, a sub-optimal solution of 29 experiments out of 324 possible combinations (3^4*2^2) was selected. This choice was also led by the experimental effort that was needed to perform the synthesis and the analysis. To study the experimental variability, 3 replicates were chosen trough the D-Optimal by addition strategy, useful for selecting the best informative condition within the proposed experimental matrix.

The data analysis was performed in R environment through the software CAT (Chemometric Agile Tool). The 32 experiments available to estimate 26 coefficients (6 degree of freedom) are listed in table 9 and are reported in the randomized execution order.

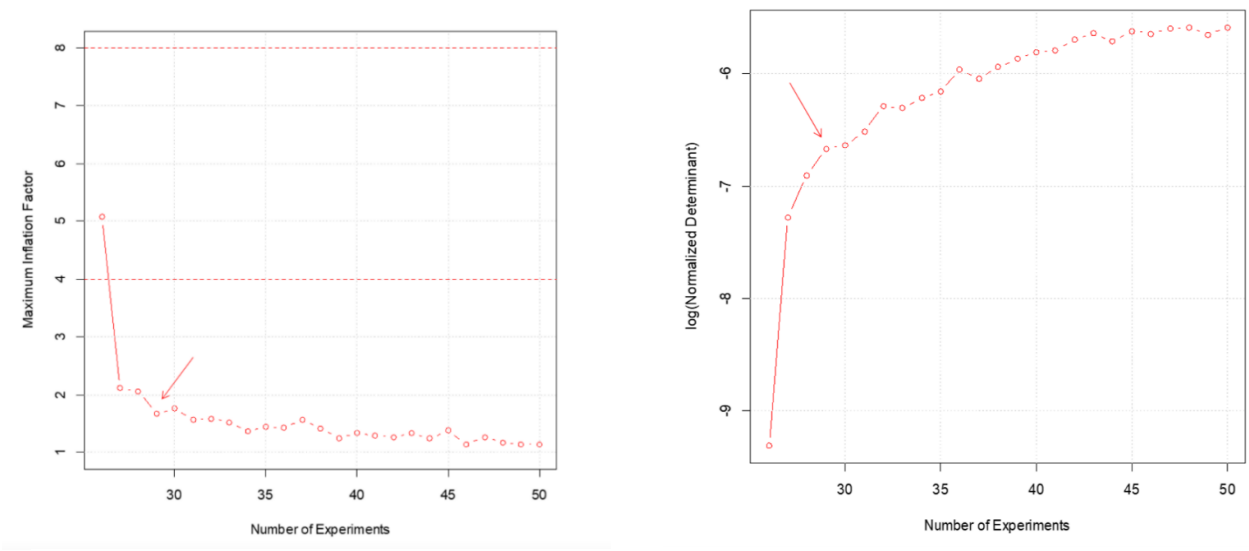

Figure 20. Normalized determinant (left) and inflation factor (right) chart; Each chart has number of experiments on x axis; Normalized determinant has log (normalize determinant) on x axis, while inflation factor has maximum inflation factor value.

Table 9. List of the performed 32 experiments.

Exp	Coded						Actual						Rep.
	Oleoresin (mg)	Lipid chemical structure	Lipid (mg)	Surfactant chemical structure	Surfactant (mg)	Water (ml)	Oleoresin (mg)	Lipid chemical structure	Lipid (mg)	Surfactant chemical structure	Surfactant (mg)	Water (ml)	
1	1	-1	0	-1	-1	-1	300	Compritol	400	Lecithin 50	60	8	
2	1	1	0	1	0	1	300	Stearic acid	400	Lecithin 75	90	15	r1
3	1	1	-1	-1	1	-1	300	Stearic acid	350	Lecithin 50	120	8	
4	1	1	-1	1	-1	-1	300	Stearic acid	350	Lecithin 75	60	8	
5	-1	-1	0	1	0	1	100	Compritol	400	Lecithin 75	90	15	
6	-1	-1	-1	1	-1	-1	100	Compritol	350	Lecithin 75	60	8	
7	-1	1	1	-1	1	-1	100	Stearic acid	450	Lecithin 50	120	8	
8	1	-1	-1	1	0	0	300	Compritol	350	Lecithin 75	90	11	
9	0	1	1	-1	0	-1	200	Stearic acid	450	Lecithin 50	90	8	
10	1	-1	1	-1	1	1	300	Compritol	450	Lecithin 50	120	15	r2
11	1	-1	-1	-1	-1	1	300	Compritol	350	Lecithin 50	60	15	
12	-1	1	-1	-1	-1	-1	100	Stearic acid	350	Lecithin 50	60	8	r3
13	-1	1	-1	1	1	-1	100	Stearic acid	350	Lecithin 75	120	8	
14	-1	-1	-1	-1	1	1	100	Compritol	350	Lecithin 50	120	15	
15	-1	1	-1	-1	-1	-1	100	Stearic acid	350	Lecithin 50	60	8	r3
16	1	-1	1	1	-1	1	300	Compritol	450	Lecithin 75	60	15	
17	1	-1	-1	1	1	1	300	Compritol	350	Lecithin 75	120	15	
18	1	-1	1	-1	1	1	300	Compritol	450	Lecithin 50	120	15	r2
19	1	-1	1	1	0	-1	300	Compritol	450	Lecithin 75	90	8	
20	1	1	1	-1	-1	0	300	Stearic acid	450	Lecithin 50	60	11	
21	0	-1	-1	-1	1	-1	200	Compritol	350	Lecithin 50	120	8	
22	-1	1	1	-1	-1	1	100	Stearic acid	450	Lecithin 50	60	15	
23	-1	-1	1	1	1	-1	100	Compritol	450	Lecithin 75	120	8	
24	-1	1	1	1	1	1	100	Stearic acid	450	Lecithin 75	120	15	
25	-1	1	0	-1	1	1	100	Stearic acid	400	Lecithin 50	120	15	
26	0	1	-1	1	1	1	200	Stearic acid	350	Lecithin 75	120	15	
27	-1	1	1	1	-1	-1	100	Stearic acid	450	Lecithin 75	60	8	
28	1	1	0	1	0	1	300	Stearic acid	400	Lecithin 75	90	15	r1
29	1	1	1	1	1	-1	300	Stearic acid	450	Lecithin 75	120	8	
30	-1	1	-1	1	-1	1	100	Stearic acid	350	Lecithin 75	60	15	
31	0	1	0	1	-1	0	200	Stearic acid	400	Lecithin 75	60	11	
32	-1	-1	1	-1	-1	0	100	Compritol	450	Lecithin 50	60	11	

Experimental design – CCD. A second optimization process was carried out considering the most relevant variables selected through the previous experiment design. It was shown that the best percentage of encapsulation was reached with Compritol as a lipid chemical structure, meanwhile the chemical structure, and surfactant quantity doesn't affect the results at all. For this reason, Compritol was chosen to fix the lipid chemical structure, fixing the chemical structure and quantity of surfactant using 90 mg of PHOSAL® 50 SA+.

Resulting from the above, three variables were selected for a second optimization procedure. In this case, the approach was changed to consider the variables not as their absolute values, but in ratio as described below.

$$X_1 = \text{Oleoresin (mg)}$$

$$X_2 = \frac{\text{Compritol (mg)}}{\text{Oleoresin (mg)}} = \text{lipid ratio}$$

$$X_3 = \frac{\text{Water (ml)}}{\text{Compritol+Oleoresin (mg)}} * 1000$$

Variable one may vary between 100 and 200 mg of oleoresin; Variable two is the ratio between the quantity of lipid (Compritol) and variable one (quantity of oleoresin), might be 2, 3 or 4. While variable three is the ratio between water phase volume and total amount of lipids (Compritol plus Oleoresin) multiplied by 1000. The synthesis procedure previously explained was kept the same for each experiment.

Table 10: List of variables with relative levels that have been identified as relevant to the system ("W" stands for water phase, "lipid" stands for the sum of oleoresin quantity and Compritol quantity)

		Levels		
Var. ID	Variable name	-1	0	1
X1	Oleoresin (mg)	100	150	200
X2	Lipid ratio	2	3	4
X3	W/(lipid)*1000	20	25	30

As previously described, to study the effect of the above-mentioned variables, the experimental plan was chosen according to the experimental design (DoE) approach. Following this method, it was possible to obtain a higher quality of information than can be obtained starting from a reduced experimental effort. According to the variable and their respectively values listed in table 10, the postulated multilinear regression (MLR) model, including 10 coefficients (1 constant, 3 linear terms, 3 interactions and 3 quadratic terms) is as follows:

$Y = b_0 + b_1X_1 + b_2X_2 + b_3X_3 + b_{12}X_1X_2 + b_{13}X_1X_3 + b_{23}X_2X_3 + b_{11}X_1^2 + b_{22}X_2^2 + b_{33}X_3^2$

Y = response

b_0 = constant

b_1 = linear term (oleoresin quantity)

b_2 = linear term (lipid ratio)

b_3 = linear term (Water/(lipid)*1000)

b_{12} = interaction (oleoresin quantity- lipid ratio)

b_{13} = interaction (oleoresin quantity- Water/(lipid)*1000)

b_{23} = interaction (lipid ratio - Water/(lipid)*1000)

b_{11} = quadratic term (oleoresin quantity)

b_{22} = quadratic term (lipid ratio)

b_{33} = quadratic term (Water/(lipid)*1000)

To estimate these terms a centered central composite design (CCD) was chosen, with 3 replicates of the central point, leading to a total of 17 experiments reported in table 11 in a randomized execution order.

Table 11: List of the 17 experiments performed system ("W" stands for water phase, "lipid" stands for the sum of oleoresin quantity and Compritol quantity).

Exp.	Coded			Actual			Rep.
	Oleoresin	Lipid ratio	W/total lipid*1000	Oleoresin	Lipid ratio	W/total lipid*1000	
1	0	0	0	150	3	25	r
2	1	1	-1	200	4	20	
3	0	0	-1	150	3	20	
4	-1	-1	-1	100	2	20	
5	0	1	0	150	4	25	
6	1	-1	1	200	2	30	
7	-1	-1	1	100	2	30	
8	1	-1	-1	200	2	20	
9	0	0	0	150	3	25	r
10	0	0	1	150	3	30	
11	-1	0	0	100	3	25	
12	-1	1	1	100	4	30	
13	-1	1	-1	100	4	20	
14	0	-1	0	150	2	25	
15	1	1	1	200	4	30	
16	0	0	0	150	3	25	r
17	1	0	0	200	3	25	

5.3 Results and discussion.

In order to ensure the antioxidant properties of lycopene the NLCs were prepared containing Exenia oleoresin. A preliminary test was performed following a procedure already applied by the Laboratory for Vascular Translational Science, Cardiovascular Bioengineering. A preliminary synthesis of NLCs was performed to evaluate the feasibility of this and the affecting experimental parameters. The same protocol was applied to synthesise NLCs containing sunflower seed oil taken as an example of traditional lipidic phase. The average particle size of NLCs containing oleoresin was 139 nm (figure 21, right), while the average z-potential value was -9,14 mV (figure 22, right). Analogously, the average particle size of NLCs containing sunflower seeds oil resulted to be 130 nm (figure 21, left), while the average z-potential value was -6,84 mV (figure 22, left). The lycopene percentage of entrapment was of around 46% and the α-TEAC value of 1,352. Based on these promising results an experimental design was set to minimize the number of experiments necessary to optimize the NLCs synthesis, maximizing the percentage of entrapment oleoresin and exploring how the particle size distribution may vary.

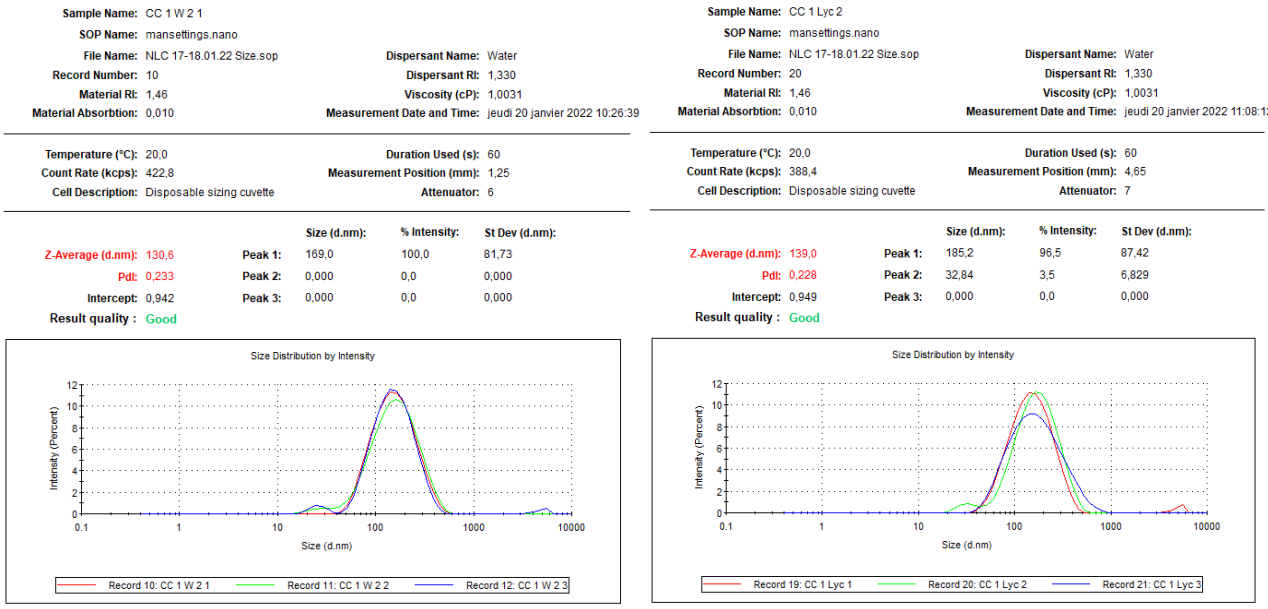

Figure 21. Particle size analysis: on the left the analysis for the sunflower oil based NLCs; on the right the analysis for Exenia oleoresin based NLCs.

Figure 22. z-potential analysis: on the left the analysis for the sunflower oil based NLCs; on the right the analysis for Exenia oleoresin based NLCs.

After running all the experiments listed in table 9 and collecting the results, they were processed in R environment through CAT software (Chemometric Agile Tool) (Leardi, Melzi, Polotti), from this processing it was possible to obtain the coefficient for the equation of the postulated model, and the value for residual standard deviation and explained variance.

Stars represent the statistical significance (p-value; * = 0.05, ** = 0.01, *** = 0.001).

$$\text{Encapsulation (\%)} = 58.81 - 19.44X_1\ (***) - 8.47X_2\ (**) - 0.55X_3 + 0.35X_4 + 0.53X_5 + 3.99X_6 + 0.71X_1X_2 + 0.16X_1X_3 - 0.18X_1X_4 - 1.78X_1X_5 + 2.86X_1X_6 - 4.56X_2X_3 + 1.89X_2X_4 - 0.90X_2X_5 - 2.89X_2X_6 + 1.47X_3X_4 - 2.90X_3X_5 - 0.18X_3X_6 + 1.65X_4X_5 + 1.66X_4X_6 - 1.68X_5X_6 - 0.51X_1^2 - 2.84X_3^2 - 2.90X_5^2 + 0.37X_6^2$$

Residual standard deviation (6 d.o.f.): 8.92; % explained variance: 78.88

The experimental variability was assessed through a pooled standard deviation, which gave an acceptable result of 3.92, estimated with 3 degrees of freedom. Since the residual standard deviation and the experimental standard deviation were not significantly different, there is no *lack of fit*. As shown in figure 23, the linear terms of oleoresin (X_1) and chemical structure of lipid (X_2) are significant (X_1 at $p<0.001$; X_2 at $p<0.01$).

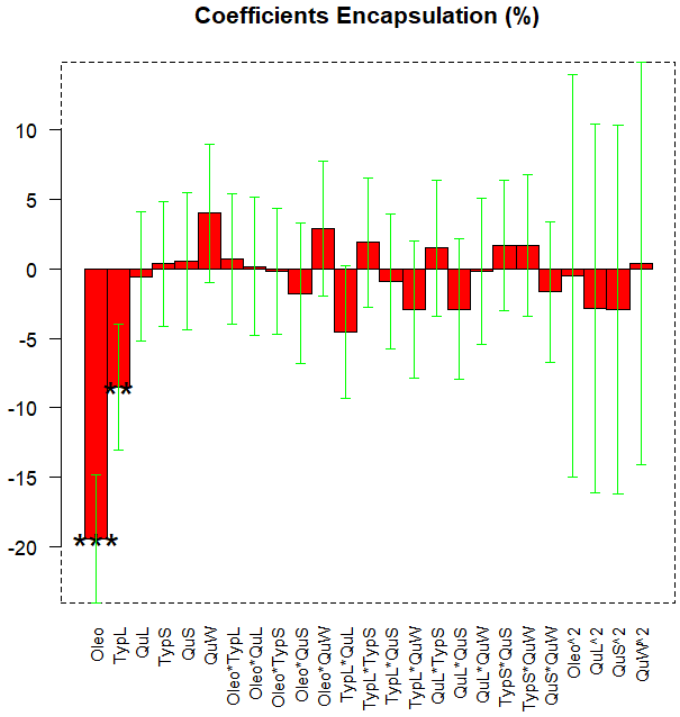

*Figure 23. Coefficients plot for the response Encapsulation % (the green bracket is the confidence interval at p=0.05, **=p<0.01, ***=p<0.001).*

The linear terms show that the highest encapsulation percentages are achieved at low quantity of oleoresin and with Compritol. The interaction X_2X_3 is close to the statistical significance, therefore the response surface will be further analysed.

The response surface in figure 24 is shown in the plane of the variable's chemical lipid structure (X_2) and lipid quantity (X_3) by setting the oleoresin variable (X_1) at level

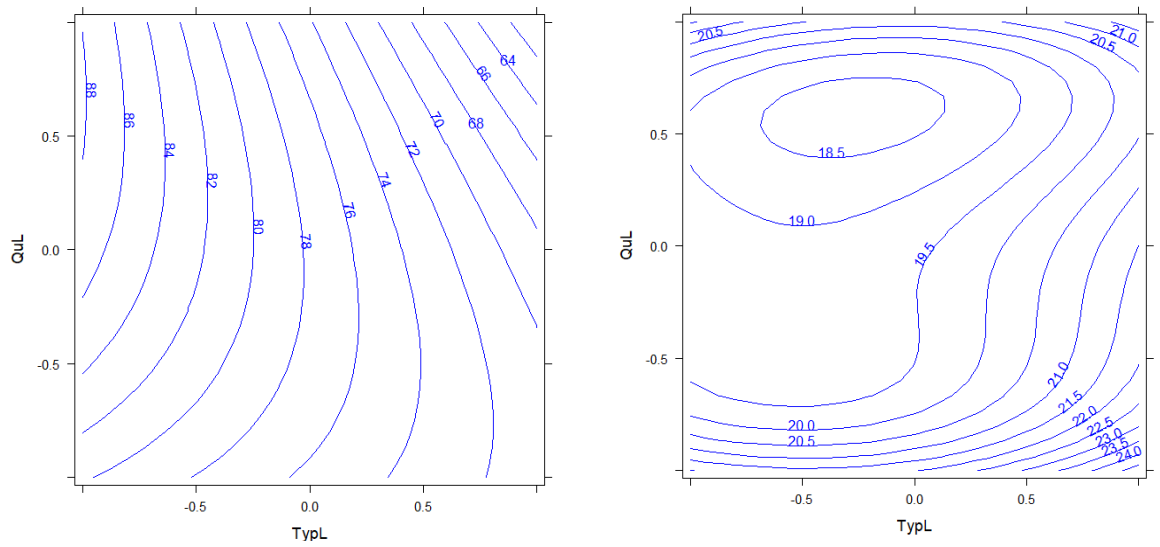

Figure 24. Contour plot for response Encapsulation % (left), and semi amplitude of the confident interval (right) for interaction chemical structure of lipid and quantity of lipid.

-1 and the other variables at level 0, together with its semiamplitude of the confidence interval. It is possible to interpret the interaction (close to the statistical significance): by working with a higher amount of lipid (X_3 at lev.+1) the effect of the chemical structure (X_2) is greater than working at lower amount (X_3 at lev.-1). The best encapsulation percentage is obtained with Compritol (X_2 at lev.-1) at its highest quantity (X_3 at lev.+1).

Furthermore, the particle size distribution of the NLCs was analysed. Despite the use of the common "descriptors" (D10, D50, D90 of the cumulative curve), a multivariate analysis of the whole particle size distribution was computed. All the 32 experiments were analysed in triplicate after centrifugation. The results were averaged since the analytical variability was lower than the imposed variability. The dataset useful for the elaboration is composed of the 32 experiments described by 25 diameter classes (diameter classes from 28.2-32.7 to 955.4-1106 nm).

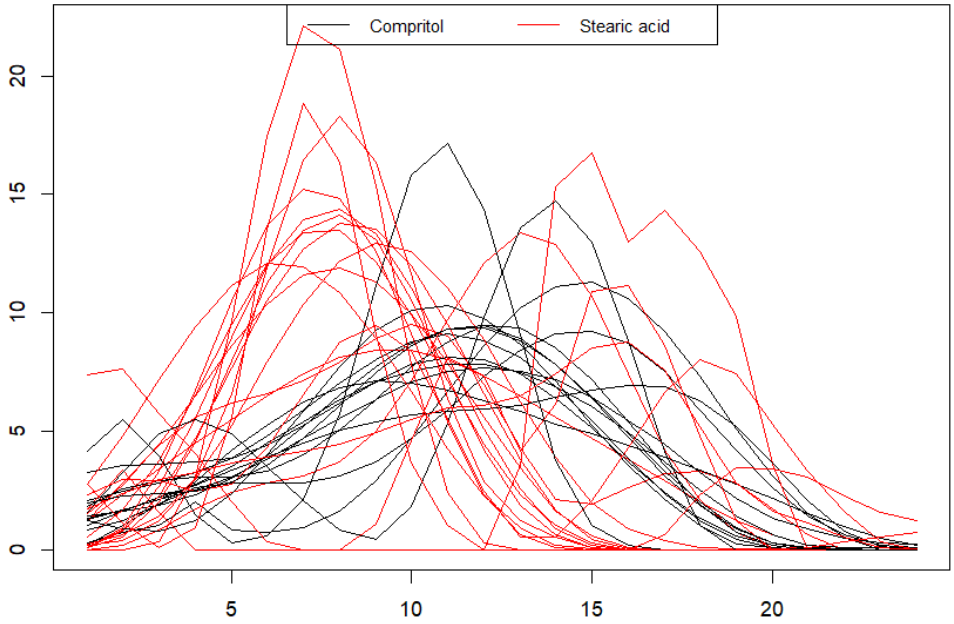

Figure 25. Graphic representation of particle size distribution for each sample (on x axis is represented the 25 diameter class, while on y axis the quantity of particle in the specific diameter class).

Figure 25 shows the particle size distribution of the samples. In the plot the samples are coloured according to the chemical structure of lipid (var. X_2), where it is possible to see the great effect connected to this variable: the use of Compritol (black lines in figure 25) leads to particles with a larger particle size associated with a wider distribution than the stearic acid. Within this data matrix, a principal components

analysis was performed (PCA). As in this case where the data is obtained are rather noisy, the PCA is important to extract the useful information from the noise within the data.

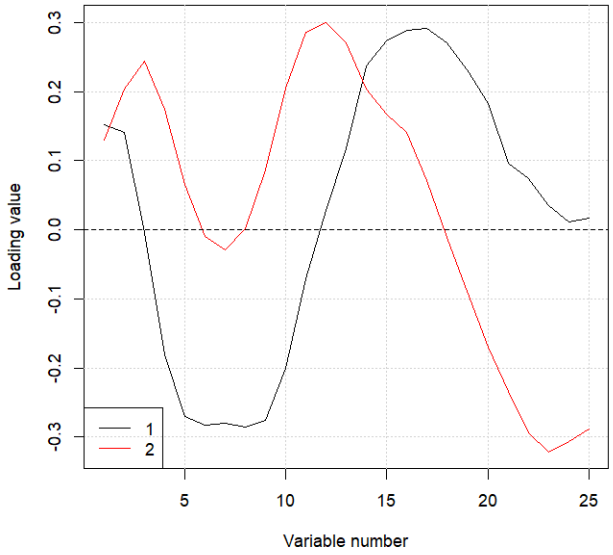

Figure 26. Line loading plot of PC1 and PC2.

The PCA, after autoscaling, identifies two significant components that explain respectively 33.96% and 27.29% of the variance (in total 61.3%).

To interpret the principal components the line loading plot is showed where the loadings are plotted along the 25 diameter classes. The first principal component (PC1, black line) explains the average of the particle diameter. Samples characterized by negative scores have finer particles, while samples characterized by positive scores have particles with a larger particle size. Instead, PC2 explains the residual shape information of the distributions, not considered at this stage.

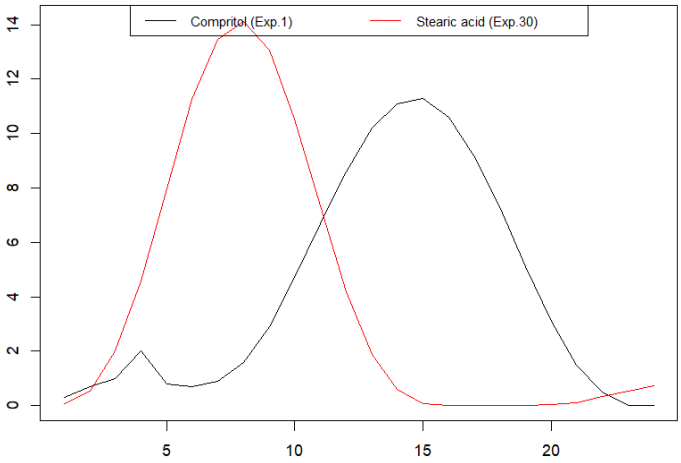

Figure 27. Graphic representation of two samples with opposite scores on PC1 and similar scores on PC2 (on x axis is represented the 25-diameter class, while on y axis the quantity of particle in the specific diameter class).

To visually understand the physical meaning of PC1, two samples with opposing scores on PC1 and similar scores on PC2 are plotted: exp.1 (positive scores on PC1) is shifted towards higher diameter sizes; on the contrary, exp.30 (negative scores on PC1) is shifted towards lower diameter sizes and therefore it has finer particles.

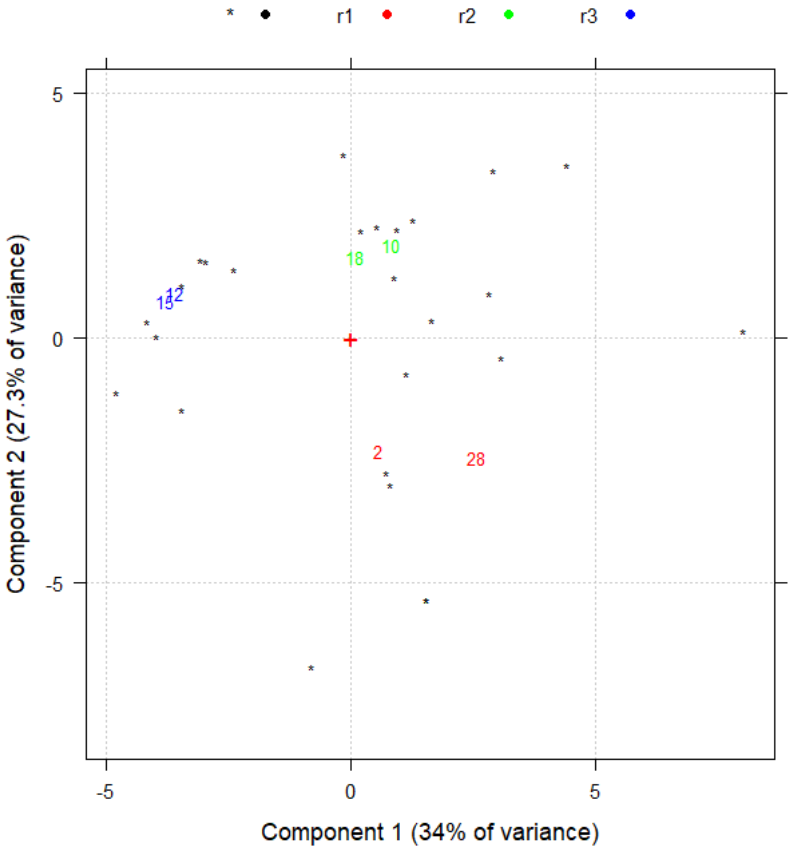

Figure 28. Score plot on plane PC1-PC2 (61,3% of total variance).

The score plot in the plane PC1-PC2 is shown in figure 28, highlighting the three pairs of replicates in order to visually assess the experimental variability. It is possible to notice that the experimental variability is definitively lower than the imposed variability. The PC1 scores (average particle size) were used as a response to compute the MLR model. To simplify the interpretation, the score values were scaled on a range from 0 to 100, where 0 meant the finest particle size and 100 meant the coarsest particle size.

Average particle size = $43.44 + 8.25X_1 - 6.52X_2 + 2.42X_3 - 0.85X_4 - 0.67X_5 - 1.73X_6 + 11.23X_1X_2$ (*) $- 3.51X_1X_3 - 0.47X_1X_4 - 0.75X_1X_5 - 0.95X_1X_6 - 0.91X_2X_3 + 1.05X_2X_4 + 6.84X_2X_5 - 3.88X_2X_6 - 0.21X_3X_4 + 4.24X_3X_5 - 4.27X_3X_6 + 3.46X_4X_5 + 0.38X_4X_6 + 2.99X_5X_6 - 23.94X_1^2 + 19.08X_3^2 - 18.37X_5^2 + 19.53X_6^2$

% Explained variance: 46.63

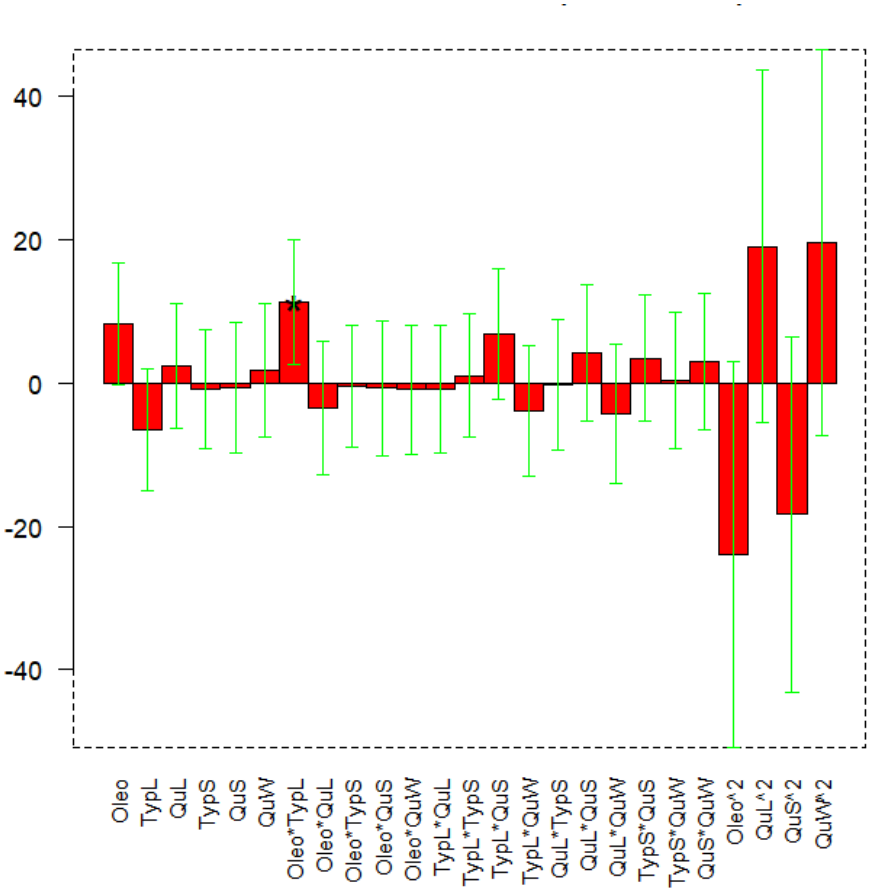

*Figure 29. Coefficients plot for scores in PC1 (the green bracket is the confidence interval at p=0.05, *=p<0.05).*

The interaction between oleoresin and chemical structure of lipid is significant (X_1X_2) with a $p<0.05$, thus the response surface will be analysed.

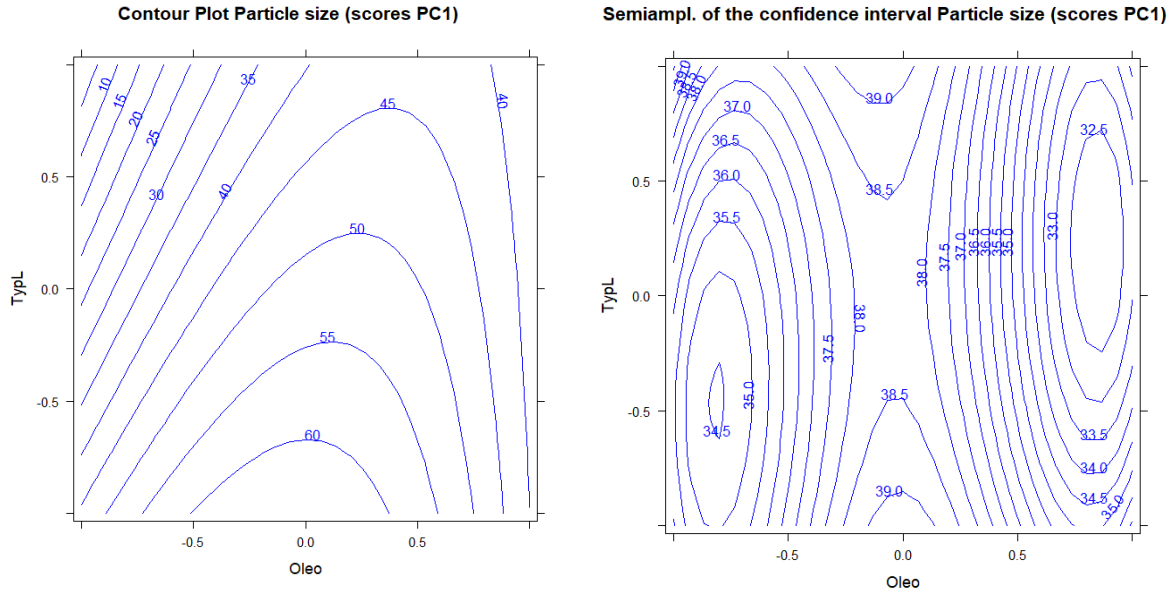

Figure 30. Contour plot for response Particle size (left), and semi amplitude of the confident interval (right) for interaction oleoresin and chemical structure of lipid.

The response surface in figure 30 is shown in the plane of oleoresin (X_1) and chemical structure of lipid (X_2) variables by setting the other variables at level 0, together with its semiamplitude of the confidence interval. It is possible to notice that working with smaller quantity of oleoresin, the experiments obtained using stearic acid (X_2 at lev.-1) are characterized by finer particles, while the use of Compritol results in particles with a larger particle size. By increasing the quantity of oleoresin, the particles become coarser and coarser. Further investigation will be conducted to understand the role of particle size to better select the best size.

Based on the results obtained through the D-optimal design it has been decided to run a second optimization process, which was carried out considering the most relevant variables selected through the previous experiment design. It has shown that the best percentage of encapsulation was reached with Compritol as a lipid chemical structure, meanwhile the chemical structure, and quantity of surfactant doesn't affect the results at all. For this reason, Compritol was chosen to fix the lipid chemical structure and quantity of surfactant using 90 mg of PHOSAL® 50 SA+. Resulting from that, three variables have been selected for a second optimization procedure based on a CCD design and previously described. After running all the experiments listed in table 11

and collecting the results, they have been processed in R environment through CAT software (Chemometric Agile Tool) (Leardi, Melzi, Polotti), after this processing is possible to obtain the coefficient for the equation of the postulated model, and the value for residual standard deviation and explained variance.

Encapsulation %; (to be maximized) = $59.53 - 18.39X_1$ (***) $- 11.18X_2$ (**) $- 4.14X_3 - 1.27X_1X_2 - 1.20X_1X_3 + 2.13X_2X_3 + 3.31X_1^2 - 0.30X_2^2 + 0.31X_3^2$

Stars represent the statistical significance (p-value; * = 0.05, ** = 0.01, *** = 0.001).

Residual standard deviation (7 d.o.f.): 10.07; % explained variance: 71.13

The experimental variability was assessed through a pooled standard deviation, which gave an acceptable result of 6,69, estimated with 2 degrees of freedom. Since the residual standard deviation and the experimental standard deviation were not significantly different, there is no *lack of fit*.

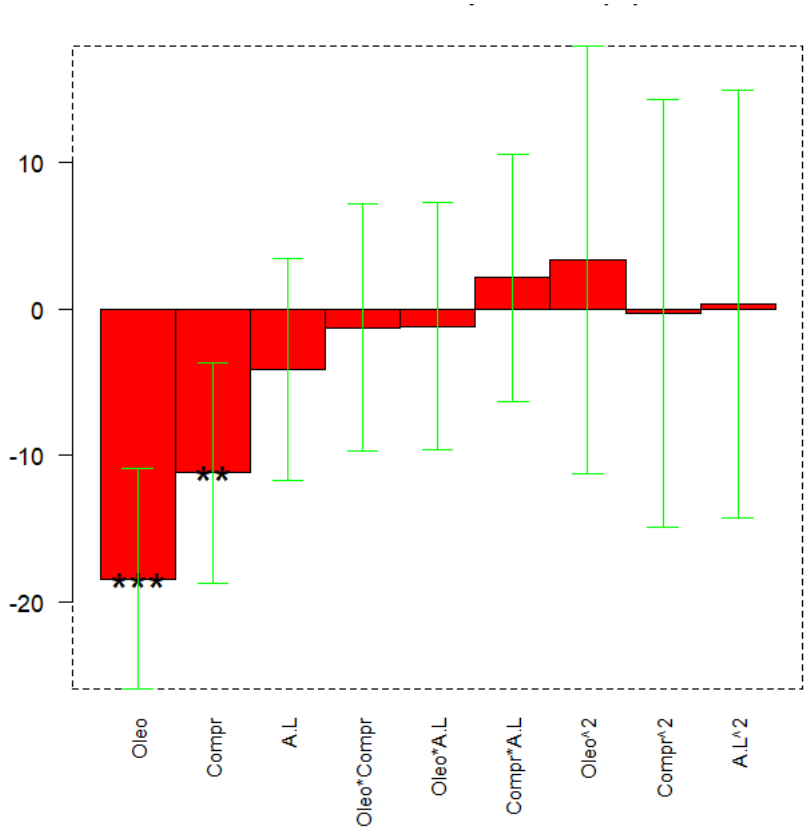

*Figure 31. Coefficients plot for the response Encapsulation % (the green bracket is the confidence interval at p=0.05, **=p<0.01, ***=p<0.001).*

As shown in figure 31 the linear terms for oleoresin (X_1) and lipid ratio (X_2) variables are significant (X_1 at $p<0.001$; X_2 at $p<0.01$). The linear terms show that the highest encapsulation percentage is achieved with lower amounts of oleoresin and with lower ratios of Compritol to oleoresin.

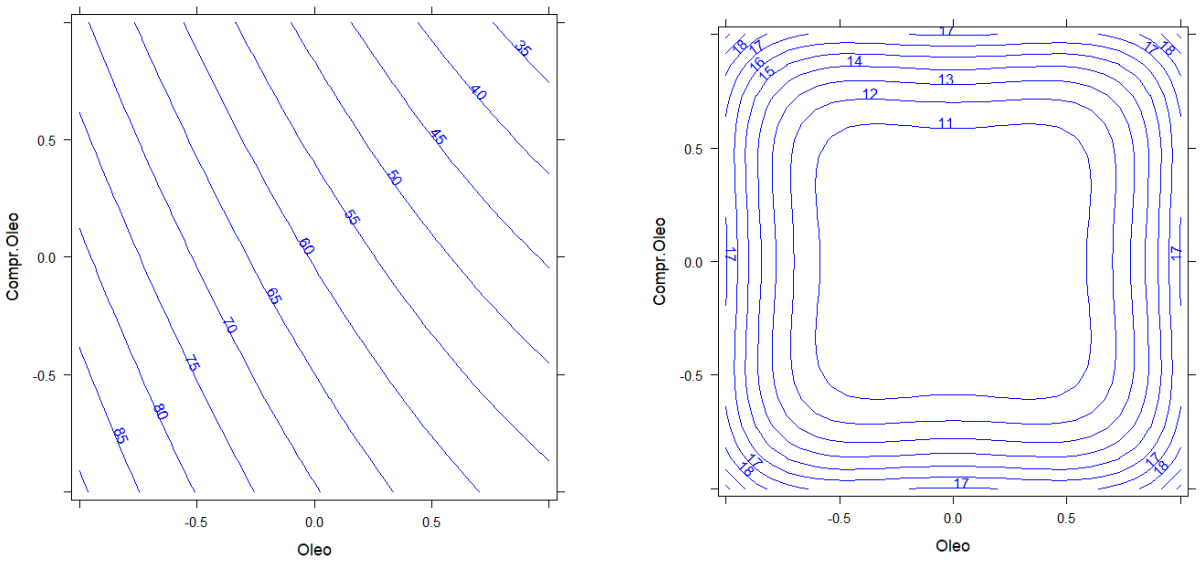

Figure 32. Contour plot for response Encapsulation % (left), and semi amplitude of the confident interval (right) for interaction oleoresin and ration of oleoresin to Compritol

The response surface (figure 32) is shown in the plane quantity of oleoresin (X_1) and ratio of oleoresin to Compritol (X_2) variables by setting the ratio of aqueous phase to lipid phase variable (X_3) at level 0, together with its semiamplitude of the confidence interval. It is possible to notice that working with smaller quantities of oleoresin and smaller ratios of oleoresin to Compritol result in a better encapsulation. Again, the particle size distribution on the 17 samples was analysed in duplicate, hence the dataset useful for the elaboration is made up of the 32 experiments described by 25 diameter classes (diameter classes from 11.7-13.5 to 1718-1990 nm). The PCA, after autoscaling, identifies 3 significant components that explain respectively 48.0%, 20.7% and 16.5% of the variance (in total 85.2%). However, the first significant component only, that explains the average particle size, was considered: the scaled PC1 scores were used as a response to compute the MLR model (0 means the finest particle size and 100 means the coarsest particle size).

Average particle size = $28.67 + 20.46X_1 + 23.62X_2 + 6.01X_3 + 10.58X_1X_2 - 3.23X_1X_3 + 0.17X_2X_3 + 19.87X_1^2 + 0.52X_2^2 - 15.12X_3^2$

% explained variance: 66.67

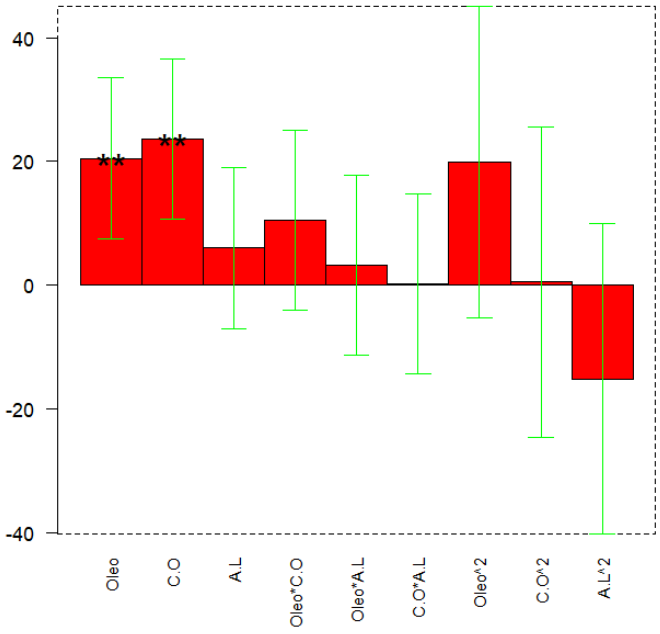

*Figure 33. Coefficients plot for the response particle size (the green bracket is the confidence interval at p=0.05, **=p<0.01).*

The linear terms for oleoresin (X_1) and ratio of oleoresin to Compritol (X_2) variables are significant ($p<0.01$) (figure 33). The linear terms show that the finest particles are achieved with lower amounts of oleoresin and lower ratios of Compritol to oleoresin.

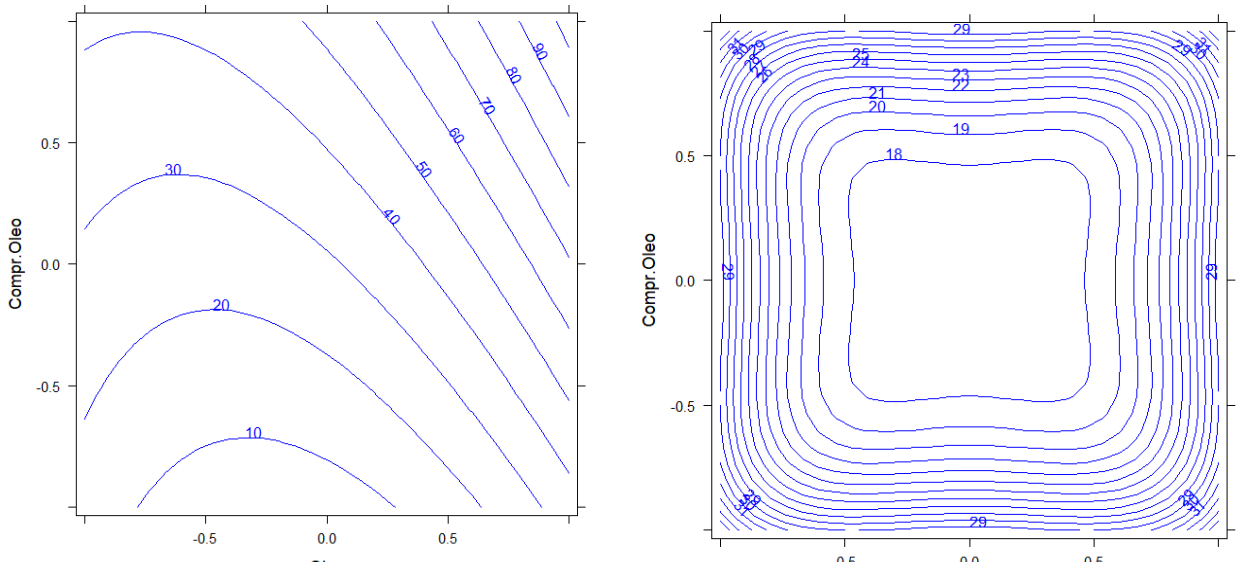

Figure 34. Contour plot for response Particle size (left), and semi amplitude of the confident interval (right) for interaction oleoresin and ratio oleoresin/Compritol.

By studying the same response surface (figure 34), it is possible to notice that by working with higher quantities of oleoresin brings to particles with a larger particle size, especially with higher ratios of oleoresin to Compritol. Comparing the two responses (% encapsulation with respect to particle size) the negative correlation is clear, in which the smallest particles are also those with the highest encapsulation performance.

The goal of this piece of work was reached, since it has been possible to maximize the percentage of encapsulation at 98 % performing 49 experiments rather than the 341, required from an univariate approach. In literature, similar nanoparticles have been obtained with an average yield percentage of 51% by spry drying process (Nunes, and Mercadante, 2007) meanwhile freeze-dry methodology gives back a higher value, close to 84% (Souza, et al., 2018). The preliminary synthesis of NLCs with the methodology applied in our work, gives a comparable result with the one obtained by Nunes, and Mercadante (2007), however a better result has been obtained thanks to the optimization through the experimental design. Furthermore, it was possible to form an idea about variable affect particle size distribution and how it works. Further study will investigate the role of particle size in the absorption of these NLCs from the intestinal system, and thanks to this work, whic has already studied the variables that affect this parameter, it would be possible to synthesize NLCs which are more suitable for intestinal adsorption.

Antioxidant properties. The inhibition curves for Exenia oleoresin, lycopene standard and NLCs are reported in figure 35 - 37. Comparing the slopes of the straight lines obtained for the Exenia oleoresin and for α-tocopherol (slope of straight line equal to 0,928) a value of α-TEAC equal to 3,016 was obtained that suggests the higher antioxidant activity of the Exenia oleoresin which also appeared more active than lycopene standard whose α-TEAC value resulted equal to 0,737. The difference between the antioxidant activity of Exenia oleoresin and standard lycopene can result from the presence of some other compounds in the Exenia oleoresin that have antioxidant activity, but also from a synergic effect in those compounds and lycopene. Further investigations will be performed.

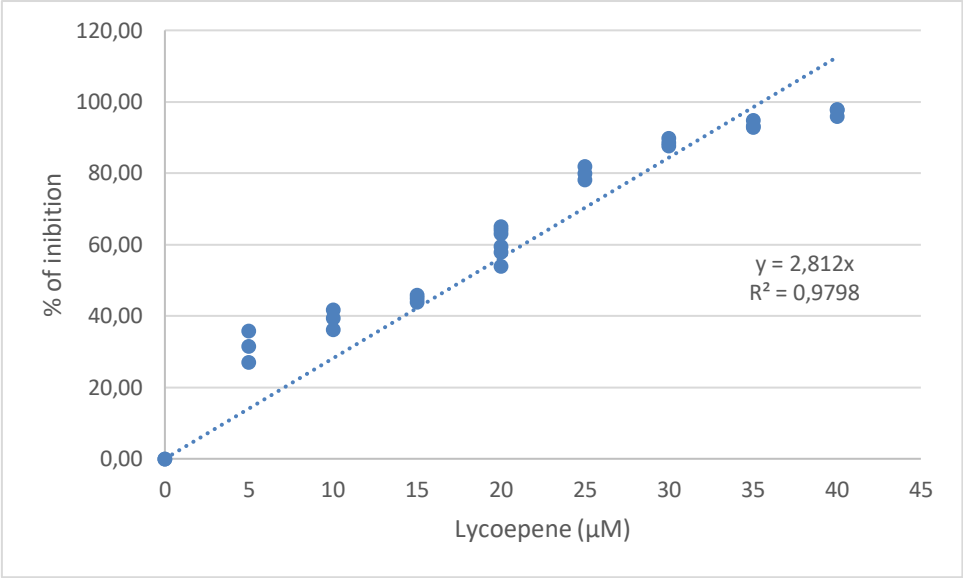

Figure 35. Inhibition curve for Oleoresin.

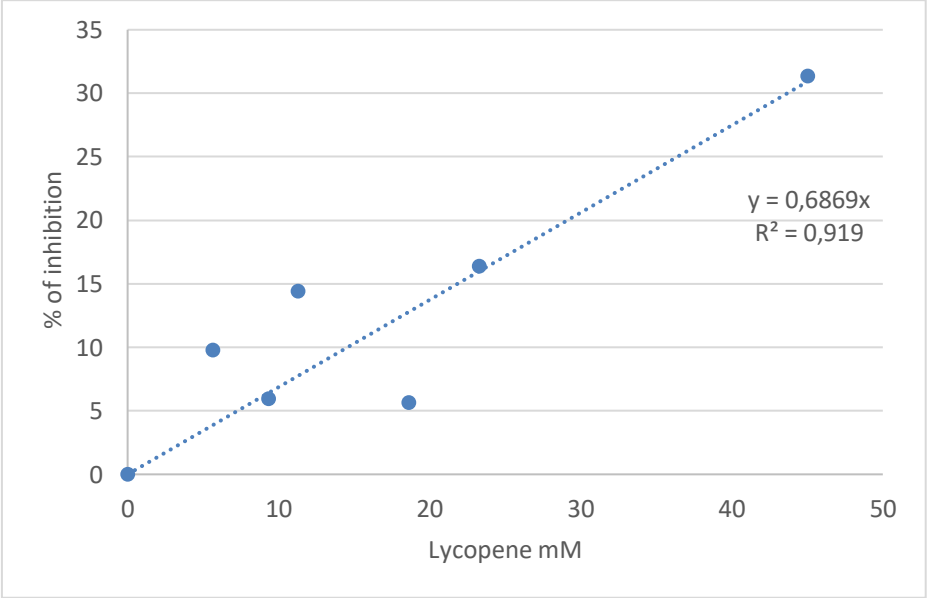

Figure 36. Inhibition curve for lycopene standard.

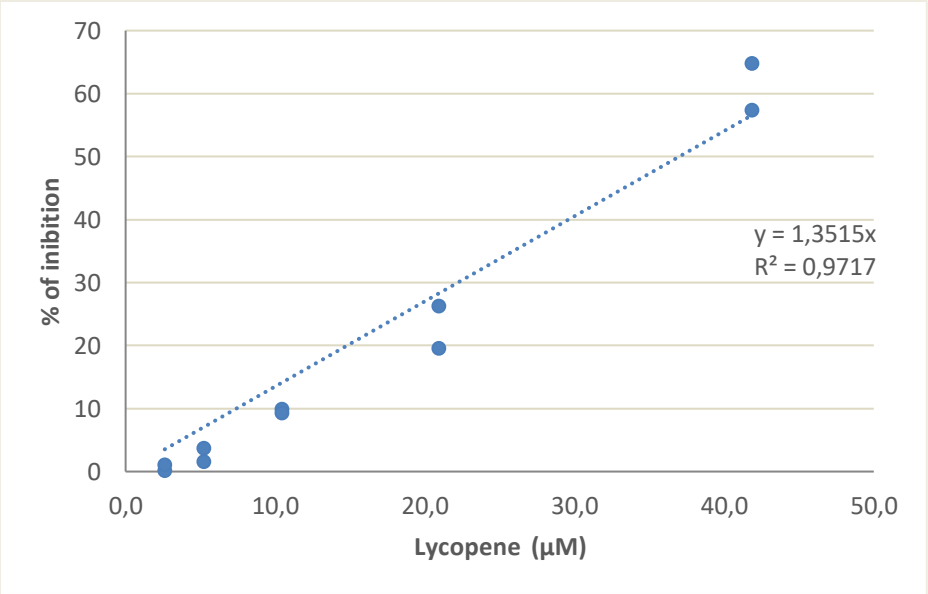

Figure 37. Inhibition curve for NLCs.

The slope of the straight lines of an inhibition curve obtained for NLCs containing lycopene (figure 37) resulted in about double that of the slope of the straight line of the inhibition curve obtained for the for α-tocopherol which suggested high antioxidant activity despite an entrapment of lycopene in NLCs being equal to about 46%.

The oleoresin analysed and used in the present research comes from an industrial extraction research project of by-products and has a relatively low lycopene content and shows a higher antioxidant activity compared to standard lycopene alone, following the ABTS assay. This property has been maintained also after the encapsulation on NLCs. The NLCs synthesis step was fundamental to valorising the extract obtained from the waste material through a green extraction technique, supercritical carbon dioxide extraction, since lycopene, due to its intrinsic nature, is quite unstable to oxidants, light, and temperature. As a mean as to obtain the best results possible from the NLCs synthesis process, an experimental design technique allowed to select the conditions to reach the highest percentage of encapsulation and at the same time to monitor the particle size distribution. This approach allowed the study of the effects of the six parameters in a first screening step, underlining which one was actually affecting the result in the study domain. Once the screening design pointed out which variable affects the result in the studied domain, the study moved to a second experiment design to improve the variable range suitable for the chosen

goal. From this study it is possible to say that in the studied domain, the best result for encapsulation percentage were reached with oleoresin at a lower level and Compritol at lower ratio with oleoresin. On the contrary, surfactant chemical structure and quantity didn't affect the results at all, nor the water phase quantity or the ratio either. This approach allowed also to us have an idea about which variable affects particle size distribution and how it works. This opportunity was appreciated since it was not possible to predict which specific composition particle size gives the best results in the intestinal adsorption. Further study will clarify the role of the NLCs particle size in the intestinal adsorption and so it may be possible to optimise the synthesis conditions in order to obtain the most performant product.

Conclusions.

This research project conjugated the green technology present in Exenia group, supercritical carbon dioxide extraction methodology, with the knowledge of analytical methodology and the opportunities that the network of universities can offer. In the first year, the extraction process of *Amaranthus cruentus* seeds was developed. Market needs emerged within Exenia stimulated the interest in this raw material. The use of a univariate approach led to process parameters that combine high extraction yield with the containment of energy consumption. Performing the extraction at 350 bars and 50°C, and collecting the extract after the first 120 minutes, obtained an oil with high content of squalene (about 15% of oil weight). If the extraction was carried out for further 150 minutes, another fraction of oil was obtained with a lower squalene content, whichwas suitable for sale in the food or cosmetic market due to the biological properties of oil.

In the second year, the research moved to the valorisation of tomato waste material as source of lycopene, a well known antioxidant food additive. Due to the desire to explore as many variables as possible using the lowest possible number of experiments to minimize experimentation times and costs, a multivariate approach based on a design of experiment was applied. The study evidenced the importance of the conditionas under which the tomatoes were harvested. The waste coming from tomatoes harvested in summer gave the best yield if the supercritical carbon dioxide extraction is performed at 350 bars and flow rate of 24 kg/h, while the temperature doesn't affect it, and can be set at minimum value to minimize energy consumption (60°C). If the waste comes from spring harvested tomatoes instead, also the temperature affects the yields, and so it is necessary to work at high explored temperature (80°C), and at 350 bars with a flow of 24 kg/h.

The first, and second-year approaches were different: a univariate one for *Amaranthus cruentus* and a multivariate one for the tomatoes. The multivariate path allowed us to manage several variables simultaneously, including the nature of the raw material, and relative interactions. The knowledge problem is explored more deeply with a significant reduction of experimental time and cost.

Lycopene, due to its intrinsic nature, is quite unstable to oxidants, light, and temperature. To valorise the lycopene oleoresin obtained during the second year, the

last year of the doctorate focused on the synthesis of nanoparticle lipidic carriers (NLCs). Also in this case, the research followed an experimental design approach that allowed the selection of the process conditions in order to reach the highest yield of lycopene containing oil encapsulation and, at the same time, to monitor the nanoparticles size distribution. However, the role of nanoparticle size distribution in intestinal adsorption is as yet unknown, so this study is an original contribution to the greater work of selecting the best conditions for the synthesis of NLCs and to tune their size distribution.

References

Ashraf, W., Latif, A., Zhang, L., Zhang, J., Wang, C, Rehman, A., Hussain, A., Siddiquy, M., Karim, A. (2020). Technological Advancement in the Processing of Lycopene: A Review. Food Rev. Int., 38, 1–27.
https://doi.org/10.1080/87559129.2020.1749653.

Armenta, S., Garrigues, S., Esteve-Turrillas, F.A., de la Guardia, M., 2019. Green extraction techniques in green analytical chemistry. TrAC Trends Anal. Chem. 116, 248–253.
https://doi.org/10.1016/j.trac.2019.03.016

Arts M.J.T. J., Dallinga J. S., Voss HP., Haenen G.R.M.M., Bast A.; A new approach to assess the total antioxidant capacity using the TEAC assay, Food Chemistry, Volume 88, Issue 4, 2004, 567-570.
https://doi.org/10.1016/j.foodchem.2004.02.008.

Barba A, Hurtado MC, Mata M, Ruiz VF, Tejada M., 2006. Application of a UV–Vis detection-HPLC method for a rapid determination of lycopene and β-carotene in vegetables. Food Chem., 95, 328–336.
https://doi.org/10.1016/j.foodchem.2005.02.028.

Benincá, C., Ortiz, R.W.P., Gonçalves, F.F., Martins, M.L., Mangrich, A.S., Zanoelo, E.F., 2016. Pressure cycling extraction as an alternative to percolation for production of instant coffee. Sep. Purif. Technol. 164, 163–169.
https://doi.org/10.1016/j.seppur.2016.03.032

Bhuiya, M.M.K., Rasul, M., Khan, M., Ashwath, N., Mofijur, M., 2020. Comparison of oil extraction between screw press and solvent (n-hexane) extraction technique from beauty leaf (Calophyllum inophyllum L.) feedstock. Ind. Crops Prod. 144, 112024.
https://doi.org/10.1016/j.indcrop.2019.112024

Bukhanko, N., Attard, T., Arshadi, M., Eriksson, D., Budarin, V., Hunt, A.J., Geladi, P., Bergsten, U., Clark, J., 2020. Extraction of cones, branches, needles and bark from Norway spruce (Picea abies) by supercritical carbon dioxide and soxhlet extractions techniques. Ind. Crops Prod. 145, 112096.
https://doi.org/10.1016/j.indcrop.2020.112096

Borges Silva, L., Lourenco, P., Teixeira, A., Azevedo, E.B., Alves, M., Elias, R.B., Silva, L., 2018. Biomass valorisation in the management of woody plant invaders: The case of Pittosporum undulatum in the Azores. Biomass Bioenergy 109, 155–165. https://doi.org/10.1016/j.biombioe.2017.12.025

Bucić-Kojić, A., Planinić, M., Tomas, S., Bilić, M., Velić, D., 2007. Study of solid–liquid extraction kinetics of total polyphenols from grape seeds. J. Food Eng. 81, 236–242.
https://doi.org/10.1016/j.jfoodeng.2006.10.027

Cadoni E., Giorgi M.R., Medda E., Poma G. (2000). Supercritical CO2 extraction of lycopene and β-carotene from ripe tomatoes. Dyes and Pigments, 44(1), 27-32. https://doi.org/10.1016/S0143-7208(99)00065-0.

Calderon-Jacinto R., Matricardi P., Gueguen V., Pavon-Djavid G., Pauthe E. and Rodriguez-Ruiz V.. Dual Nanostructured Lipid Carriers/Hydrogel System for Delivery of Curcumin for Topical Skin Applications. Biomolecules 2022, 12, 780. https://doi.org/10.3390/biom12060780.

Chan, C.-H., Yusoff, R., Ngoh, G.-C., Kung, F.W.-L., 2011. Microwave-assisted extractions of active ingredients from plants. J. Chromatogr. A 1218, 6213–6225. https://doi.org/10.1016/j.chroma.2011.07.040

Chemat, F., Rombaut, N., Meullemiestre, A., Turk, M., Perino, S., Fabiano-Tixier, A.-S., Abert-Vian, M., 2017. Review of Green Food Processing techniques. Preservation, transformation, and extraction. Innov. Food Sci. Emerg. Technol. 41, 357–377. https://doi.org/10.1016/j.ifset.2017.04.016

Chen, Y.P., Gu, Y.F., Zhao, H.R., Zhou, Y.M., 2021. Dietary squalene supplementation alleviates diquat-induced oxidative stress and liver damage of broiler chickens. Poult. Sci. 100, 100919.
https://doi.org/10.1016/j.psj.2020.12.017

Choudhari, SM., Ananthanarayan, L. (2007). Enzyme aided extraction of lycopene from tomatoes tissues. Food Chemistry, 102(1), 77-81.
https://doi.org/10.1016/j.foodchem.2006.04.031

Czitrom, V., 1999. "One-Factor-at-a-Time Versus Designed Experiments". American Statistician. 53 (2): 126–131. https://doi.org/10.2307/2685731

Costa-Rodrigues, J.; Pinho, O.; Monteiro, P.R.R. (2018). Can Lycopene Be Considered an Effective Protection against Cardiovascular Disease? Food Chemistry, 245, 1148–1153.
https://doi.org/10.1016/j.foodchem.2017.11.055.

Daniel, C. (1973),"One-at-a-Time Plans," Journal of the American Statistical Association 68, 353-360

Das, I., Arora, A., 2021. Kinetics and mechanistic models of solid-liquid extraction of pectin using advance green techniques- a review. Food Hydrocoll. 120, 106931.
https://doi.org/10.1016/j.foodhyd.2021.106931

de Jesus, S.S., Filho, R.M., 2020. Recent advances in lipid extraction using green solvents. Renew. Sustain. Energy Rev. 133, 110289.
https://doi.org/10.1016/j.rser.2020.110289

de Melo, M.M.R., Silvestre, A.J.D., Silva, C.M., 2014. Supercritical fluid extraction of vegetable matrices: Applications, trends and future perspectives of a convincing green technology. J. Supercrit. Fluids 92, 115–176.
https://doi.org/10.1016/j.supflu.2014.04.007

Eggleton T., A short introduction to climate change, Cambridge university press, New York, 2013, p.52, ISBN 978-1-107-61876-3 Paperback

Fang, C., Fernie, A.R., Luo, J., 2019. Exploring the Diversity of Plant Metabolism. Trends Plant Sci. 24, 83–98.
https://doi.org/10.1016/j.tplants.2018.09.006

Ferrentino, G., Giampiccolo, S., Morozova, K., Haman, N., Spilimbergo, S., Scampicchio, M., 2020. Supercritical fluid extraction of oils from apple seeds: Process optimization, chemical characterization, and comparison with a conventional solvent extraction. Innov. Food Sci. Emerg. Technol. 64, 102428.
https://doi.org/10.1016/j.ifset.2020.102428

Friedman, M., and Savage, L. J. (1947), "Planning Experiments Seeking Maxima," in Techniques of Statistical Analysis, eds. C. Eisenhart, M. W. Hastay, and W. A. Wallis, New York: McGraw-Hill, pp. 365-372.

Gavahian, M., Sastry, S., Farhoosh, R., Farahnaky, A., 2020. Ohmic heating as a promising technique for extraction of herbal essential oils: Understanding mechanisms,

recent findings, and associated challenges, in: Advances in Food and Nutrition Research. Elsevier, pp. 227–273.
https://doi.org/10.1016/bs.afnr.2019.09.001

Gullon, P., Gullon, B., Romani, A., Rocchetti, G., Lorenzo, J.M., 2020. Smart advanced solvents for bioactive compounds recovery from agri-food by-products: A review. Trends Food Sci. Technol. 101, 182–197.
https://doi.org/10.1016/j.tifs.2020.05.007

He, H.-P., Cai, Y., Sun, M., Corke, H., 2002. Extraction and Purification of Squalene from Amaranthus Grain. J. Agric. Food Chem. 50, 368–372.
https://doi.org/10.1021/jf010918p

Hedrick J.L., Mulcahey L.J., Taylor L.T. (1992). Supercritical fluid extraction. Mikrochimica Acta, 108, 115-132.
https://doi.org/10.1007/BF01242421

Hidalgo, B; Goodman, M (2013). "Multivariate or multivariable regression?". Am J Public Health. 103: 39–40.
https://doi:10.2105/AJPH.2012.300897

Jia, C., Cao, D., Ji, S., Lin, W., Zhang, X., Muhoza, B., 2020. Whey protein isolate conjugated with xylo-oligosaccharides via Maillard reaction: characterization, antioxidant capacity, and application for lycopene microencapsulation. LWT – Food Science and Technology 118, 108837.
https://doi.org/10.1016/j.lwt.2019.108837

Jiang, T., Ghosh, R., Charcosset, C., 2021. Extraction, purification and applications of curcumin from plant materials-A comprehensive review. Trends Food Sci. Technol. 112, 419–430.
https://doi.org/10.1016/j.tifs.2021.04.015

Krulj J.,Brlek T., Pezo L., Brkljaca J., Popovic S., Zekovic Z. and Solarova M.B.. Extraction methods of Amaranthus sp. grain oil isolation. J Sci Food Agric 2016; 96: 3552–3558.
https://doi.org/10.1002/jsfa.7540

Kotz, J.C., Treichel, P.M., Townsend, J.R., 2013. Chemistry.

Kumcuoglu, S, Yilmaz, T., Tavman, S. (2014). Ultrasound assisted extraction of lycopene from tomatoes processing wastes. Journal of food sciences and technology-mysore, 51(12), 4102-4107.
https://doi.org/10.1007/s13197-013-0926-x

Leardi R. (2018), D-Optimal Designs in Encyclopedia of Analytical Chemistry: Applications, Theory and Instrumentation, 1-11. John Wiley & Sons, Ltd.
https://doi.org/10.1002/9780470027318.a9646.

Leardi R. (2009). Experimental design in chemistry: A tutorial. Analytica Chimica Acta, 652(1-2), 161-172.
https://doi.org/10.1016/j.aca.2009.06.015.

Leardi R., Melzi C., Polotti G., CAT (Chemometric Agile Tool). http://gruppochemiometria Biochemistry.it/index.php/software

Li Y.,Cui Z., Hu L.. Recent technological strategies for enhancing the stability of lycopene in processing and production. Food chemistry,405, 2023, 134799.

Lomonaco, T., Manco, E., Corti, A., La Nasa, J., Ghimenti, S., Biagini, D., Di Francesco, F., Modugno, F., Ceccarini, A., Fuoco, R., Castelvetro, V., 2020. Release of harmful volatile organic compounds (VOCs) from photo-degraded plastic debris: A neglected source of environmental pollution. J. Hazard. Mater. 394, 122596.
https://doi.org/10.1016/j.jhazmat.2020.122596

Lou, X., Guo, X., Wang, K., Wu, C., Jin, Y., Lin, Y., Xu, H., Hanna, M., Yuan, L., 2021. Phenolic profiles and antioxidant activity of Crataegus pinnatifida fruit infusion and decoction and influence of in vitro gastrointestinal digestion on their digestive recovery. LWT 135, 110171.
https://doi.org/10.1016/j.lwt.2020.110171

Lu M., Qiu Q., Luo X., Sun J., Wang C., Lin X., Deng Y., Song Y., Phyto-phospholipid complexes (phytosomes): a novel strategy to improve the bioavailability of active constituents, Asian Journal of Pharmaceutical Sciences. 2019, 14, 265-274

Mandal, V., Tandey, R., 2016. A critical analysis of publication trends from 2005–2015 in microwave assisted extraction of botanicals: How far we have come and the road ahead. TrAC Trends Anal. Chem. 82, 100–108.
https://doi.org/10.1016/j.trac.2016.05.020

Mariatti, F., Gunjević, V., Boffa, L., Cravotto, G., 2021. Process intensification technologies for the recovery of valuable compounds from cocoa by-products. Innov. Food Sci. Emerg. Technol. 68, 102601.
https://doi.org/10.1016/j.ifset.2021.102601

Mascio P.D., Kaiser S., Sies H., (1989). Lycopene as the most efficient biological carotenoid singlet oxygen quencher. Archives of and Biophysics, 274(2), 532-538.
https://doi.org/10.1016/0003-9861(89)90467-0

Machmudah S.; Zakaria, Winardi S., Sasaki M., Goto M., Kusumoto N., Hayakawa K., (2011). Lycopene extraction from tomato peel by-product containing tomato seed using supercritical carbon dioxide. J. Food Eng., 108, 290–296.
https://doi.org/10.1016/j.jfoodeng.2011.08.012

Micera M., Chemical composition and biological activity of plantderived extracts obtained by supercritical CO_2 extraction, Doctorate thesis, Torino, 2021.

Micera M., Botto A., Geddo F., Antoniotti S., Bertea C. M., Levi R., Gallo M. P. and Querio G., Squalene: more than a step towards sterols, Antioxidants, 2020.
https://doi.org/10.3390/antiox9080688

Moharrami, S., Hashempour, H., 2021. Comparative study of low-voltage electric field-induced, ultrasound-assisted and maceration extraction of phenolic acids. J. Pharm. Biomed. Anal. 202, 114149.
https://doi.org/10.1016/j.jpba.2021.114149

Nunes, I.L., Mercadante, A.Z., 2007. Encapsulation of lycopene using spray-drying and molecular inclusion processes. Braz. Arch. Biol. Technol. 50, 893–900.
https://doi.org/10.1590/S1516-89132007000500018

Ollanketo, M., Hartonen, K., Riekkola, ML., Holm, Y., Hiltunen, R., (2001). Supercriticl carbon dioxide extraction of lycopene in tomato skins, European food research and technology, 212(5), 561-565. https://doi.org/ 10.1007/s002170100298

Olkin, I.; Sampson, A. R. (2001-01-01), "Multivariate Analysis: Overview", in Smelser, Neil J.; Baltes, Paul B. (eds.), International Encyclopedia of the Social & Behavioral Sciences, Pergamon, pp. 10240–10247, ISBN 9780080430768

Özcan, M.M., Ghafoor, K., Al Juhaimi, F., Ahmed, I.A.M., Babiker, E.E., 2019. Effect of cold-press and soxhlet extraction on fatty acids, tocopherols and sterol contents of the Moringa seed oils. South Afr. J. Bot. 124, 333–337.

https://doi.org/10.1016/j.sajb.2019.05.010

Peltola, P., Pihlajamaki, J., Koutnikova, H., Ruotsalainen, E., Salmenniemi, U., Vauhkonen, I., Kainulainen, S., Gylling, H., Miettinen, T.A., Auwerx, J., Laakso, M., 2006. Visceral Obesity is Associated with High Levels of Serum Squalene*. Obesity 14, 1155–1163.

https://doi.org/10.1038/oby.2006.132

Popescu M., Iancu P., Plesu V., Todasca M.C., Isopencu G.O., Bildea C.S., (2022). Valuable Natural Antioxidant Products Recovered from Tomatoes by Green Extraction. Molecules, 27(13), 4191.

https://doi.org/10.3390/molecules27134191.

Pulok K. Mukherjee, Bioactive phytocomponents and their analysis. Pulok. K. Mukherjee Editor. Quality control and evaluation of herbal drugs. Elsevier. 2019, pp. 237-328. ISBN: 9780128133743

Pulok K. Mukherjee, Phyto-Pharmaceuticals, Nutraceuticals and Their Evaluation Pulok. K. Mukherjee Editor. Quality control and evaluation of herbal drugs. Elesevier. 2019, pp. 707-722. ISBN: 9780128133743

Ravindran R. and Jaiswal A. K., (2016). Exploitation of Food Industry Waste for High-Value Products. Trends in Biotechnology, 34, 58–69.

https://doi.org/10.1016/j.tibtech.2015.10.008

Rodriguez-Ruiz V., Salatti-Dorado J. Á., Barzegari A., Nicolas-Boluda A., Houaoui A., Caballo C., Caballero-Casero N., Sicilia D., Bastias Venegas J., Pauthe E., Omidi Y., Letourneur D., Rubio S., Gueguen V. and Pavon-Djavid G.. Astaxanthin-Loaded Nanostructured Lipid Carriers for Preservation of Antioxidant Activity. Molecules 2018, 23, 2601.

https://doi:10.3390/molecules23102601

Savatovic S., Cetkovic G., Canadanovic-Brunet J., Djlas S. (2012). Tomatoes waste: a potential source of hydrophilic antioxidant. International Journal of Food Science and Nutrition, 63(2), 129-137.

https://doi.org/10.3109/09637486.2011.606211

Schlosky K., "Supercritical phase transitions at very high pressure", 1989, J. Chem. Ed. 66 (12): 989.

https://doi.org/10.1021/ed066p989

Souza, A.L.R., Hidalgo-Chávez, D.W., Pontes, S.M., Gomes, F.S., Cabral, L.M.C., Tonon, L. V., 2018. Microencapsulation by spray drying of a lycopene-rich tomato concentrate: characterization and stability. LWT - Food Sci. Technol. (Lebensmittel-Wissenschaft -Technol.) 91, 286–292.
https://doi.org/10.1016/j.lwt.2018.01.053

Sparr Eskilsson, C., Björklund, E., 2000. Analytical-scale microwave-assisted extraction. J. Chromatogr. A 902, 227–250.
https://doi.org/10.1016/S0021-9673(00)00921-3

Vallecilla-Yepez L., Ciftici O.N. (2018). Increasing cis-lycopene content of the oleoresin from tomato processing byproducts using supercritical carbon dioxide. LWT-Food Sci. Technol., 95, 354–360.
https://doi.org/10.1016/j.lwt.2018.04.065.

Vinatoru, M., 2015. Ultrasonically assisted extraction (UAE) of natural products some guidelines for good practice and reporting. Ultrason. Sonochem. 25, 94–95.
https://doi.org/10.1016/j.ultsonch.2014.10.003

Vinatoru, M., Mason, T.J., Calinescu, I., 2017. Ultrasonically assisted extraction (UAE) and microwave assisted extraction (MAE) of functional compounds from plant materials. TrAC Trends Anal. Chem. 97, 159–178.
https://doi.org/10.1016/j.trac.2017.09.002

Wimalasiri D., Brkljaca R., Piva T. J., Urban S., Huynh T. 2017. Comparative analysis of carotenoid content in Momordica cochinchinensis (Curcurbitaceae) collected from Australia, Thailand and Vietnam, J Food Sci Technol, 2814-2824.
https://doi.org/ 10.1007/s13197-017-2719-0

Wojdyło, A., Samoticha, J., Chmielewska, J., 2021. Effect of different pre-treatment maceration techniques on the content of phenolic compounds and color of Dornfelder wines elaborated in cold climate. Food Chem. 339, 127888.
https://doi.org/10.1016/j.foodchem.2020.127888

Zhang, Z., Kang, Y., Che, L., 2019. Composition and thermal characteristics of seed oil obtained from Chinese amaranth. LWT 111, 39–45.
https://doi.org/10.1016/j.lwt.2019.05.007

Zygler, A., Słomińska, M., Namieśnik, J., 2012. Soxhlet Extraction and New Developments Such as Soxtec, in: Comprehensive Sampling and Sample Preparation. Elsevier, pp. 65–82.
https://doi.org/10.1016/B978-0-12-381373-2.00037-5